

# Multivariate Statistical Analysis of Hydrochemical and Microbiological Natural Tracers as a Tool for Understanding Karst Hydrodynamics (The Unica Springs, SW Slovenia)

Marina Ćuk Đurović, Metka Petrič, Igor Jemcov, Janez Mulec, Zdenka Mazej Grudnik, Cyril Mayaud, Matej Blatnik, Blaž Kogovšek, Nataša Ravbar



Дигитални репозиторијум Рударско-геолошког факултета Универзитета у Београду

[ДР РГФ]

Multivariate Statistical Analysis of Hydrochemical and Microbiological Natural Tracers as a Tool for Understanding Karst Hydrodynamics (The Unica Springs, SW Slovenia) | Marina Ćuk Đurović, Metka Petrič, Igor Jemcov, Janez Mulec, Zdenka Mazej Grudnik, Cyril Mayaud, Matej Blatnik, Blaž Kogovšek, Nataša Ravbar | Water Resources Research | 2022 | |

10.1029/2021WR031831

<http://dr.rgf.bg.ac.rs/s/repo/item/0006940>

Дигитални репозиторијум Рударско-геолошког факултета Универзитета у Београду омогућава приступ издањима Факултета и радovima запослених доступним у слободном приступу. - Претрага репозиторијума доступна је на [www.dr.rgf.bg.ac.rs](http://www.dr.rgf.bg.ac.rs)

The Digital repository of The University of Belgrade Faculty of Mining and Geology archives faculty publications available in open access, as well as the employees' publications. - The Repository is available at: [www.dr.rgf.bg.ac.rs](http://www.dr.rgf.bg.ac.rs)

# Water Resources Research

## RESEARCH ARTICLE

10.1029/2021WR031831

### Special Section:

Advancing process representation in hydrologic models: Integrating new concepts, knowledge, and data

### Key Points:

- A new approach to study and explain hydrodynamics of karst aquifers was developed
- It offers an innovative solution to distinguish influential monitoring parameters
- Multivariate chemographs allowed spatio-temporal detection of recharge phases

### Supporting Information:

Supporting Information may be found in the online version of this article.

### Correspondence to:

M. Čuk Đurović and N. Ravbar,  
marina.cuk@rgf.bg.ac.rs;  
natasia.ravbar@zrc-sazu.si

### Citation:

Čuk Đurović, M., Petrič, M., Jemcov, I., Mulec, J., Grudnik, Z. M., Mayaud, C., et al. (2022). Multivariate statistical analysis of hydrochemical and microbiological natural tracers as a tool for understanding karst hydrodynamics (the Unica springs, SW Slovenia). *Water Resources Research*, 58, e2021WR031831. <https://doi.org/10.1029/2021WR031831>

Received 24 DEC 2021

Accepted 12 NOV 2022

### Author Contributions:









**Conceptualization:** Marina Čuk Đurović, Metka Petrič, Igor Jemcov, Nataša Ravbar

**Data curation:** Metka Petrič, Janez Mulec, Zdenka Mazej Grudnik, Cyril Mayaud, Matej Blatnik, Blaž Kogovšek, Nataša Ravbar

© 2022. The Authors.

This is an open access article under the terms of the [Creative Commons Attribution License](https://creativecommons.org/licenses/by/4.0/), which permits use, distribution and reproduction in any medium, provided the original work is properly cited.

## Multivariate Statistical Analysis of Hydrochemical and Microbiological Natural Tracers as a Tool for Understanding Karst Hydrodynamics (The Unica Springs, SW Slovenia)

Marina Čuk Đurović<sup>1</sup> , Metka Petrič<sup>2,3</sup> , Igor Jemcov<sup>1</sup> , Janez Mulec<sup>2,3</sup> , Zdenka Mazej Grudnik<sup>4</sup>, Cyril Mayaud<sup>2,3</sup> , Matej Blatnik<sup>2,3</sup> , Blaž Kogovšek<sup>2,3</sup> , and Nataša Ravbar<sup>2,3</sup> 

<sup>1</sup>Faculty of Mining and Geology, University of Belgrade, Belgrade, Serbia, <sup>2</sup>ZRC SAZU Karst Research Institute, Postojna, Slovenia, <sup>3</sup>University of Nova Gorica, UNESCO Chair on Karst Education, Vipava, Slovenia, <sup>4</sup>Eurofins ERICo Slovenia, Ecological Research & Industrial Cooperation Ltd, Velenje, Slovenia

**Abstract** Various multivariate statistical techniques (MST) can provide valuable insights into water quality variability. Despite numerous studies in which these methods have been used, their potential has not been fully exploited. This paper presents an improved approach to better understand the hydrodynamics of karst systems. The integrated application of hierarchical cluster and principal component analysis in combination with factor analysis allowed the construction of an advanced multivariate chemograph. The analytical procedure was applied in a binary karst aquifer known for its complex hydrodynamics and mixing of water with similar hydrochemical composition. In addition, the study area provides access to an integral groundwater flow system (ponor-cave-spring) and offers extensive prior hydrogeological knowledge. The approach allowed reduction and discrimination of the main parameters affecting water quality characteristics. Their identification enabled recognition of three predominant recharge components: (a) stored water impact with Cl and electrical conductivity, (b) sinking stream impact with turbidity and bacteria composition and (c) karst aquifer impact with Ca/Mg ratio as principal parameters. The results supported innovative characterization of the dominant processes and isolation of temporal hydrodynamic phases of individual monitoring points within the aquifer system. On this basis, a spatio-temporal conceptual model was developed and the hydrodynamic behavior of the main springs was revealed. The applied methodology demonstrated to be useful in ascertaining functioning of a complex karst system under flood event conditions.

**Plain Language Summary** Karst aquifer systems contain important water resources. The quality of karst springs can deteriorate significantly after rain events, but it is difficult to distinguish how water flows and mixes in the subsurface, especially in large and complex systems. Statistical methods are powerful tools for studying these issues, but most common approaches are inadequate in some cases to reveal the origin of the water and its fate. In this paper, we present an approach in which we combined different statistical methods to explain the dynamics of water flow based on the physicochemical and microbiological properties of water. The application of these methods led to the discrimination of parameters most useful for a reliable interpretation of statistical results, such as turbidity, bacteria, Cl, EC, and Ca/Mg, and to the construction of an advanced diagram that we called a multivariate chemograph. This diagram allowed us to see where the water was coming from at any given time to our monitoring points, which allowed us to construct a detailed explanation of water flow dynamics in space and time. Our contribution is important to better predict the fate of contaminants in karst underground and to develop an early warning system for better water supply management.

## 1. Introduction

Since the 1971 study by Shuster and White (1971), hydrogeologists have used the combined interpretation of karst spring hydrographs and chemographs to infer the hydrodynamics in carbonate aquifers. The task is particularly challenging because these aquifers are characterized by a high degree of heterogeneity and discontinuity, resulting in a duality of recharge, infiltration, porosity, storage and flow (Bakalowicz, 2005; Ford & Williams, 2007; Giese et al., 2018).

The recharge conditions, together with the internal characteristics of the karst aquifer system, are the most important factors controlling water quality. Recharge can be autogenic that is, sourced entirely from precipitation that

**Formal analysis:** Marina Ćuk Đurović, Metka Petrič, Igor Jemcov, Janez Mulec, Zdenka Mazej Grudnik, Blaž Kogovšek, Nataša Ravbar

**Funding acquisition:** Igor Jemcov, Nataša Ravbar

**Investigation:** Metka Petrič, Igor Jemcov, Cyril Mayaud, Matej Blatnik, Blaž Kogovšek, Nataša Ravbar

**Methodology:** Marina Ćuk Đurović, Metka Petrič, Igor Jemcov, Nataša Ravbar

**Project Administration:** Igor Jemcov, Nataša Ravbar

**Supervision:** Metka Petrič, Igor Jemcov, Janez Mulec, Nataša Ravbar

**Validation:** Marina Ćuk Đurović, Metka Petrič, Igor Jemcov, Nataša Ravbar

**Visualization:** Marina Ćuk Đurović, Metka Petrič, Igor Jemcov, Nataša Ravbar

**Writing – original draft:** Marina Ćuk Đurović, Metka Petrič, Igor Jemcov, Janez Mulec, Zdenka Mazej Grudnik, Nataša Ravbar

falls in the karst area, and allogenic that presents runoff from non-karst rocks. Infiltration, which is an important component of recharge, occurs diffusely through soil and epikarst in the former case. It can also be concentrated via dolines or, in the latter case, through ponors that drain adjacent non-karst aquifers (Neilson et al., 2018; Williams, 2008; Worthington & Ford, 2009). Flow also depends on the type of porosity within the aquifer, resulting from the groundwater pathways that pass through the conduits, fissured systems, and the rock matrix. These differences affect the hydrogeochemical and microbiological properties of the water and have a significant impact on its quality status (Kovács et al., 2005; Vaute et al., 1997). In the fast-flowing, predominantly conduit systems, contaminants can spread rapidly and pose an increasing threat to the quality of karst springs. On the other hand, contaminants can be stored in the slow-flowing matrix systems and only a storm event can drive them toward the springs (Bicalho et al., 2010; Mahler et al., 2000).

Studies of the response of spring discharge to precipitation have proved invaluable in explaining the hydrodynamic functioning and identifying the hydraulic characteristics of karst systems (Vesper & White, 2004). Simultaneous monitoring of basic hydrochemical and microbiological parameters has often been used to provide additional hydrogeological information about water draining from karst springs (Goldscheider, 2015). The characterization of karst aquifers is a challenging task because hydraulic and spatial conduit properties are poorly defined or unknown (Reimann et al., 2011). To investigate more closely hydraulic stresses such as large recharge events, water exchange between matrix, fissures and conduits, and discharge through branched and intermeshed conduit networks (Reimann et al., 2011), it is possible to use hydrochemistry as an important method. In particular, the composition of major ions, stable isotopes, and bacteria has been considered as a natural tracer to determine the origin and mixing of different water types, transit times, and to infer hydrological or biogeochemical processes in the aquifer system (e.g., Barberá & Andreo, 2012; Chang et al., 2021; Perrin, 2003; Pronk et al., 2009; Stroj et al., 2020; Vucinic et al., 2022).

Previous studies have examined the changes in various hydrographic and hydrochemical parameters as a function of time during seasonal variations or single storm events. However, the resulting hydrographs and chemographs are limited by visual interpretation. As a result, they are not always informative with respect to potential site-specific recharge components, particularly during periods of flood events (Doctor et al., 2006; Frank et al., 2018; Winston & Criss, 2004). With modern capabilities to collect and process large data sets, multivariate statistical techniques (MST) have emerged as strong tools for studying karst aquifer dynamics and water quality variability (e.g., Bicalho, 2010; Gao et al., 2020; Moore et al., 2009). They allow the reduction of data volume, the consideration of chemical and biological parameters of different scales with equal weight, and the separation of groups of variables that share common hydrochemical properties (Fournier et al., 2007; Jiang et al., 2009; Mulec et al., 2019). Parameters such as electrical conductivity, Mg/Ca ratio, NO<sub>3</sub>, total organic carbon, turbidity, bacteria and others have been shown to be important in detecting natural processes in water-rock systems, identifying important water components, and revealing the vulnerability of the karst system to surface infiltration and anthropogenic pollution (e.g., Güler et al., 2002; Mudarra et al., 2014; Page et al., 2017).

In their review, Sánchez et al. (2015) presented the most common hydrogeochemical techniques used in karst hydrogeology. Principal component analysis (PCA) was found to be the most appropriate tool to characterize the spatial and temporal distribution of hydrochemical data and related hydrogeochemical processes. Moreover, the approach has been used to explain the hydrodynamic and hydrochemical responses of springs' behavior during a precipitation event (Mudarra & Andreo, 2011). Furthermore, hierarchical cluster analysis (HCA) has been used to provide additional insight into hydrogeological processes and water quality issues (Barbel-Périneau et al., 2019; Li et al., 2019). Jemcov and Ćuk Đurović (2020) used a combined approach of HCA and factor analysis (FA) to isolate areas with similar hydrochemical characteristics in different hydraulic regimes of a complex karst aquifer system. Various applications of single or a combination of MST are powerful tools for discriminating between components of chemically very different origins. However, such applicability is not very satisfactory in more hydrogeologically homogeneous environments.

Taking advantage of MST analysis in karst hydrogeology, this study goes a step further and develops an innovative approach to improve the characterization of karst aquifer hydrodynamics under flood event conditions. It combines HCA with PCA and FA to create a novel multivariate chemograph based on which it was possible to spatio-temporally conceptualize the functioning of a binary karst system and the hydraulic behavior of major springs. The benefit of chemographs is reflected in the ability to perform a better interpretation of karst spring data in any research area. By applying these diagrams, it is possible to make a hydrochemical-hydraulic

characterization of the predominate factors in the research area, with the ability of determining the duration of processes affecting karst spring. A well-studied karst system with a relatively uniform hydrochemical water type served as an example. Access to the integral parts of the groundwater flow system (ponors, water caves, springs), a good hydrogeological understanding of the area and known groundwater connections allowed verification of the proposed analytical procedure.

## 2. Materials and Methods

### 2.1. Study Area

The study focuses on the catchment of the Unica springs, located in southwestern Slovenia (Figures 1a and 1b). Two larger permanent springs emerge on the edge of a karst polje: Unica and Malenščica that join into the Unica River. The Malenščica spring is a regionally important drinking water source (Petrič, 2010), which drains diffusely with discharges from 1.1 to 11.2 m<sup>3</sup>/s. The Unica emerges through a network of large underground channels with discharges ranging from 0.2 to 89 m<sup>3</sup>/s (ARSO, 2020). The underground channels form a large Postojna-Planina Cave System, known worldwide for its rich biodiversity (Culver & Pipan, 2013).

The springs originate at an altitude of 448 m a.s.l. (Malenščica) and 453 m a.s.l. (Unica) and drain a binary aquifer system that extends over an area of about 820 km<sup>2</sup> and consists of three distinct recharge areas (Figure 1c): allogenic recharge of the Pivka River Basin on the west (hereafter referred to as sub-catchment A) and a chain of karst poljes on the east (referred to as sub-catchment C), and autogenic recharge from the extensive karst aquifer of the Javorniki Massif (up to an altitude of 1,796 m a.s.l.; referred to as sub-catchment B). The predominant lithology of the karst aquifer is Cretaceous rocks, mainly limestones, which in places change to dolomites and breccias. To a lesser extent, Jurassic and Paleogene carbonate rocks also occur. The same lithology extends in the southern part of the Pivka Basin forming a shallow karst aquifer. When water levels are high, surface flow occurs, receiving additional water from intermittent springs on the western foothills of the Javorniki Massif. The northern part of the Pivka Basin consists of poorly permeable Eocene flysch, which conditions a superficial river network. The Pivka River eventually sinks into the cave of Postojnska Jama.

Sub-catchment C consists of a narrow belt of karst poljes, extending along the strike-slip fault zone, and adjacent nonkarstified drainage areas. Upper Triassic dolomites predominate, changing to Jurassic limestones and dolomites to the south and west. These rocks form aquifers with fracture porosity, which in places have very poor to moderate permeability, and in some parts a superficial river network is developed. As the karst poljes follow each other in a row downgradient, they are connected in a common hydrological system with transitions between surface and groundwater flows. From the Cerknjško Polje water flows via Rakov Škocjan (as the Rak River) toward the springs of the Planinsko Polje. The alluvial sediments at the bottoms of the poljes and river valleys are of Quaternary age.

In the immediate vicinity of the Unica spring, underground streams can be reached in the cave of Planinska Jama, which is about 7 km long. In the cave two underground river channels form a unique subsurface confluence; the 2 km long channel of the Pivka River, which sinks in and flows along the cave of Postojnska Jama, is joined with the 2.5 km long channel of the Rak River, which sinks in Rakov Škocjan (Figures 1b and 1d). Together they form the Unica spring. The Rak also contributes water to the Malenščica spring. All the above groundwater flow connections were proved by tracer tests (Gabrovšek et al., 2010 and references therein). This study was conducted in six monitoring points: the contributing sinking rivers Pivka and Rak at their ponors (referred to as PP and PR), the underground channels that collect and discharge these waters in the Planinska Jama (referred to as CP and CR) and the Unica and Malenščica springs (referred to as SU and SM).

### 2.2. Meteorological and Hydrological Conditions of the Studied Flood Event Period

A typical flood event (i.e., from the onset of increased discharge to its peak and back to base level), caused by precipitation events following a long dry period, was sampled at short intervals for water quality analyses (Figure 2). The dry period lasted for several months, followed by a period of abundant precipitation between 2 November and 2 December 2019. A total of 376.8 mm of rain fell at the Postojna meteorological station, which is more than twice the average November amount during 1981–2011 (ARSO, 2021). Between 2 and 7 November, about 90 mm fell. The rainfall period was sufficiently abundant and persistent to saturate the entire aquifer, not

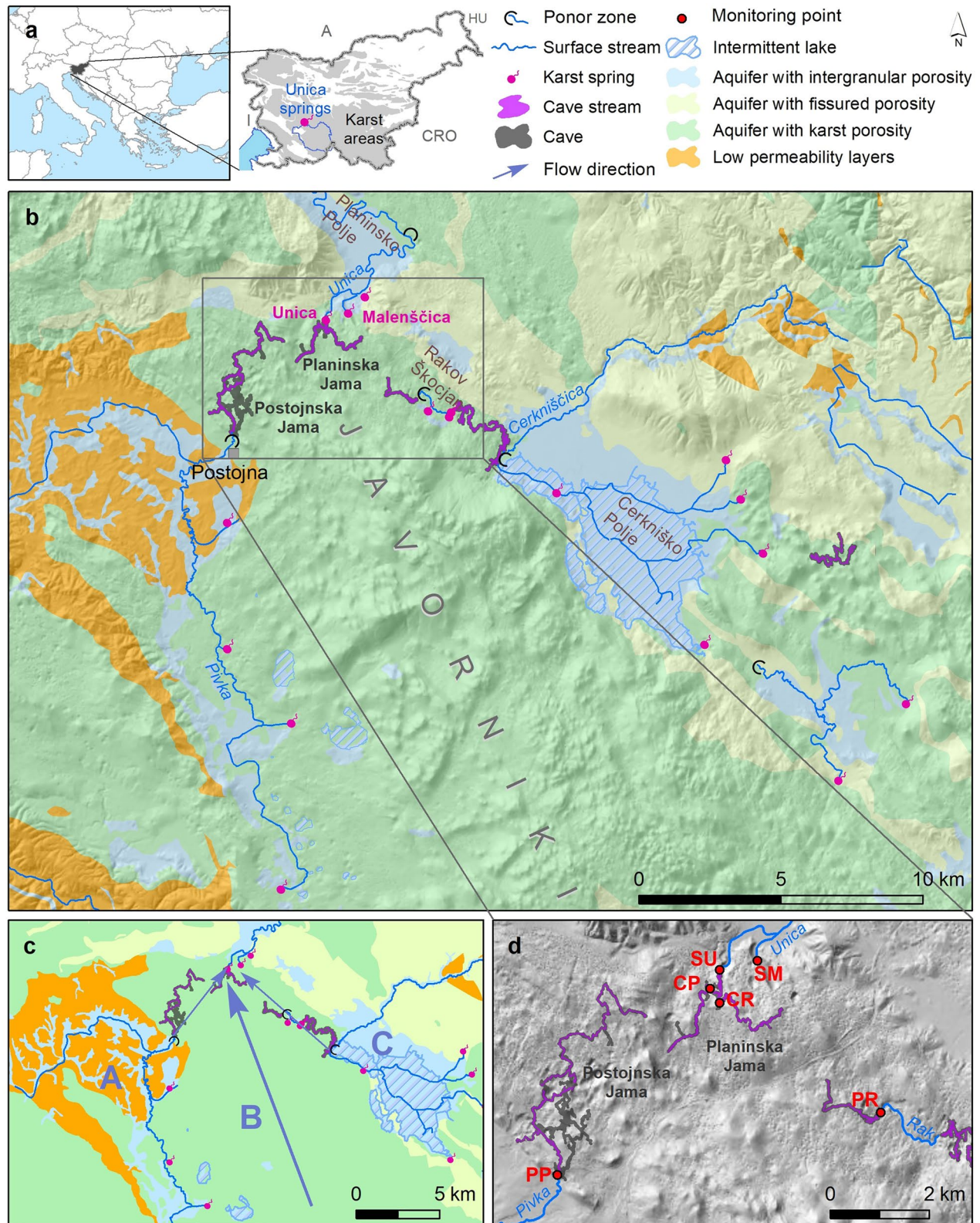


**Figure 1.** (a) Location and (b) hydrogeological situation of the study area, (c) schematic presentation of the sub-catchments (A, B, C in blue script) and general groundwater flow directions, (d) location of monitoring sites, zoomed rectangle in map b (red dots; PP—ponor of the Pivka River, PR—ponor of the Rak River, CP—Pivka and CR—Rak channels of the Planinska Jama, SU—Unica spring, SM—Malenščica spring).

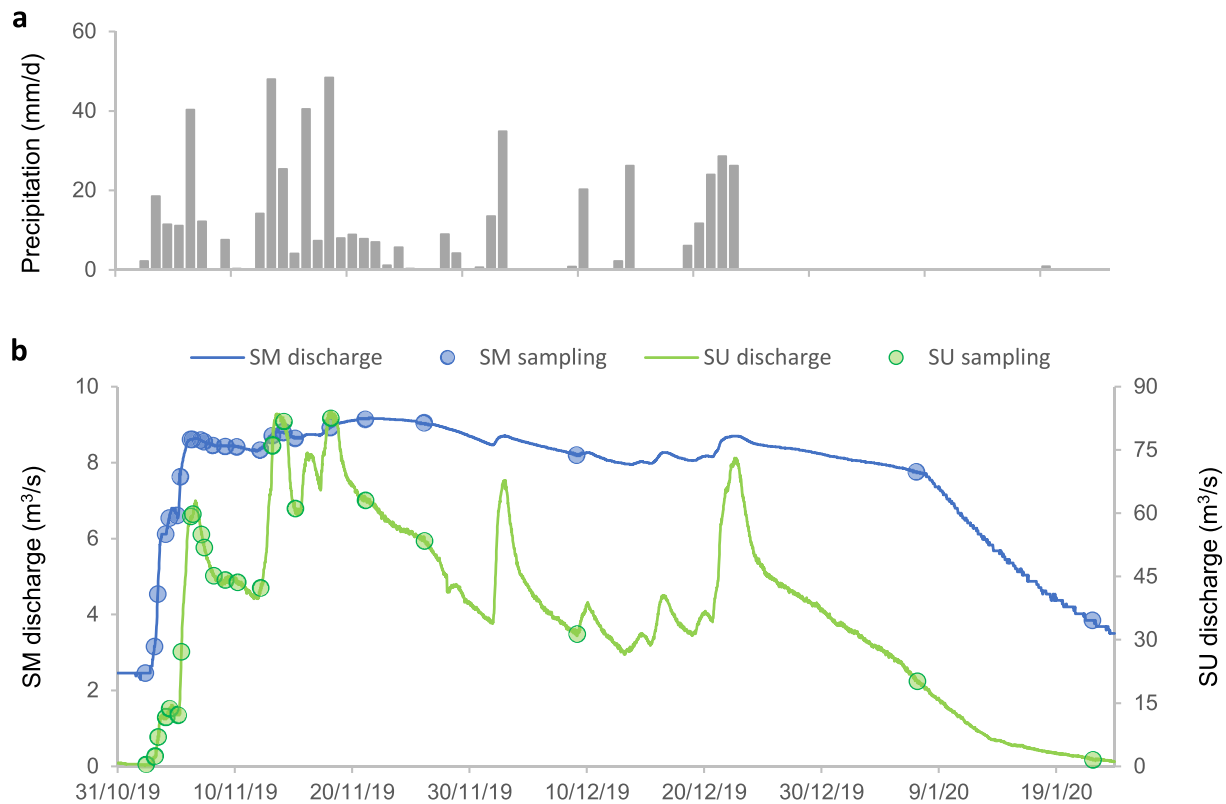


**Figure 2.** (a) Daily precipitation at Postojna meteorological station and (b) discharges of Malenščica spring (SM) and Unica spring (SU) in the period from November 2019 to January 2020. The points on the discharge curves indicate the time of sampling.

just the primary drainage pathways (conduits). Subsequently, between 12 and 18 November a total of 178.8 mm fell with a maximum intensity of 95 mm in 62 hr.

The rainy period resulted in flood event conditions with several peak discharges. The discharge of the Malenščica increased from an initial 2.5 to 8.6 m<sup>3</sup>/s on 6 November and that of the Unica from 0.5 to 62.5 m<sup>3</sup>/s on 7 November and to 83.2 m<sup>3</sup>/s on 13 November.

Detailed sampling was carried out between 2 November 2019 and 22 January 2020 (Figure 2). Samples were collected twice daily before and during intense and abundant flood events in November. Later, the sampling frequency was reduced.

### 2.3. Field and Laboratory Measurements

At the time of sampling, temperature ( $T$ ), electrical conductivity (EC) and pH were measured in the field with WTW MultiLine Multi 3620 IDS. A total of 144 samples were collected for analysis of hydrochemical and microbiological parameters. Chemical analyses were performed by Eurofins ERICo, which is accredited in accordance with SIST EN ISO/IEC 17025:2017. Parameters were measured in accordance with standard procedures using Dionex ion chromatography system ICS 3000 (ISO 10304-1: 2007/Cor 1:2010 modif.—NO<sub>3</sub>, SO<sub>4</sub>, Cl), Agilent Inductively coupled plasma mass spectrometry ICP-MS 7800c (SIST EN ISO 17294-2:2017 modif.—Ca, Mg, Na), Perkin Elmer Atomic Absorption Spectrophotometry (K) and HACH UV/VIS spectrometry (SIST ISO 7150-1:1996—NH<sub>4</sub>), Metrohm Titrino 702 SET/MET titrations (HCO<sub>3</sub>), Shimadzu TOC analyzer (SIST ISO 8245: 2000—total organic carbon) and HACH spectrophotometer (SIST EN ISO 7027:2000—turbidity).

Microbiological analysis was carried out in the laboratory of the Karst Research Institute. Microbial biomass in the water samples was estimated by two indicators. The ATP content (total microbial biomass including live and dead microbes) was estimated using AquaSnap Total testing instruments (Hygiena) and expressed in RLU—Relative Light Units (where 1 RLU equates to 1 fmol of ATP) per milliliter. Ready-to-use microbiological media

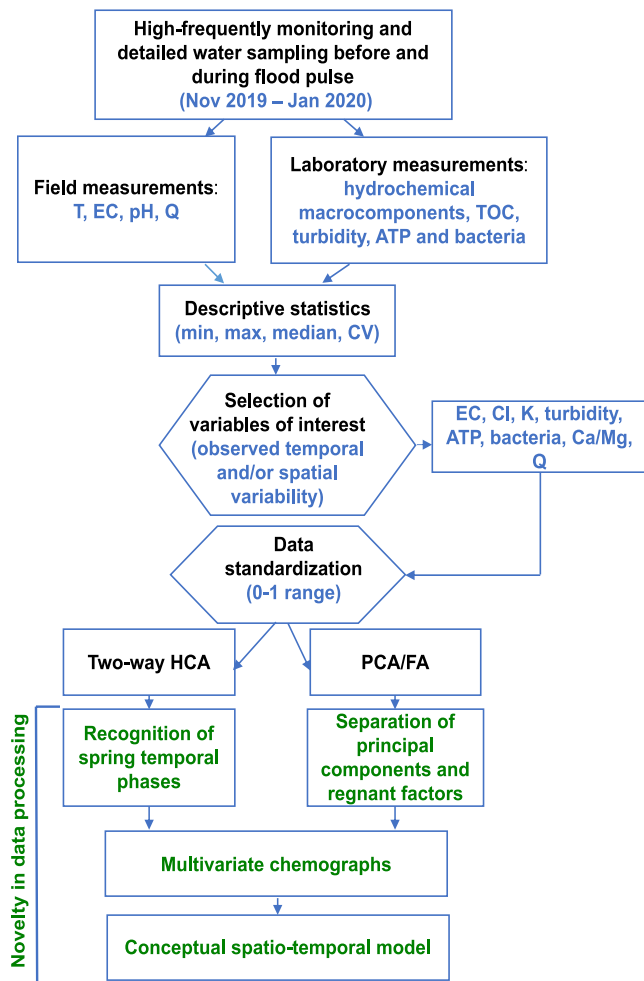


**Figure 3.** Flowchart of implemented methods and procedures that resulted in the formation of a conceptual model. General procedures are shown in black script, while the specifics for this study are shown in blue script, the actions that led to the novelty in data processing are indicated in green script.

a matrix of distances between all pairs of samples, while *R*-mode analysis calculates distances (similarities) between all pairs of variables, allowing the grouping of elements according to their associations and similar processes (Holland, 2006). Clustering performed in this manner allows for easier visual identification of separate groups through the distance graph, shown beneath the dendrogram. The place when the distance graph changes from a level slope to a sharp slope is an indication of the numbers to include. HCA enabled easier interpretation of the temporal phases that occur, through the grouping of water samples with similar hydrochemical properties, as well as the monitoring of the prevailing parameters during the considered event. Two-way dendrogram provides the possibility of considering changes in hydrochemical parameters with changes in discharge.

To achieve a detailed interpretation of the hydrochemical and microbiological spatio-temporal data, a PCA with FA was performed. PCA and FA are commonly applied to extract associations between water chemical variables and to delineate a few indicator factors responsible for variations in water quality (Singh et al., 2004). Since the research area presents a unique karst system, where the processes are interconnected and water transport could be considered from the input components (ponors), through control points (underground karst channels) to output components (karst springs), it was necessary to perform a single PCA, to study the joint action of the factors in the area, and to find out a common hydrochemical-hydraulic behavior of a system. The technique is based on the extraction of eigenvalues and eigenvectors from the covariance matrix of the original variables (Benhamiche et al., 2016; Brown, 1998). Bartlett's test was performed to test whether the correlation matrix for a data set is the

Compact Dry TC (Nissui Pharmaceutical) were used to estimate the concentration of heterotrophic aerobic bacteria. Numbers of grown bacteria were expressed as Colony-Forming Units (CFU) per milliliter after 48 hr of cultivation at 37°C.

Daily precipitation data from Postojna meteorological station and discharge values from Malenščica spring (SM) and water levels from the ponor of the Pivka River (PP) at 30-min intervals were obtained from Slovenian Environment Agency (ARSO, 2020). Onset HOBO, type U20 was used to measure and record water levels at SU at 30-min intervals. Discharges from the SU and PP were measured occasionally (22 measurements at SU and 30 at PP) at various hydrologic conditions using SonTek's FlowTracker2 and RiverSurveyor M9 to define the stage-discharge relations. Based on these relations and water level measurements, discharges from SU and PP were defined at 30-min intervals.

#### 2.4. Set Up of Multivariate Statistical Techniques Analytical Procedure

The overall data analysis included several standard statistical procedures, but the combination of performed analysis and the way of interpreting the results led to the construction of new multivariate chemographs which formed the final spatio-temporal conceptual model of the research area (Figure 3). The first step was the field and laboratory work, as described in Section 2.3. After obtaining the results, descriptive statistical analysis was applied to find the basic statistical parameters of the data and to select significant variables for multivariate analysis.

In preparing the data for multivariate statistical analysis, standardization to *z*-cores were applied as recommended by Brown (1998). A *z*-score is used for standardizing scores on the same scale by dividing a score's deviation by the standard deviation in a data set, enabling the comparison of scores that are from different units was rescaled to a range of 0–1 to have equal weight for the HCA purposes (Demlie et al., 2007). HCA was conducted using Ward's linkage method and Euclidean distance (Massart & Kaufman, 1983). Two-way HCA was performed by clustering the water samples as cases (*Q*-mode clustering) and the chemical analyses as variables (*R*-mode clustering), resulting in a two-way dendrogram. *Q*-mode analysis calculates

identity matrix (Bartlett, 1954). The Kaiser criterion (Kaiser, 1960) was applied to determine the total number of components for each data set in this analysis. Components with eigenvalues greater than or equal to 1 were extracted using PCA, for which a varimax rotation was performed by FA. Orthogonal projection according to the Varimax rotation technique is commonly used in the FA procedure (Davis, 1973). Factor loadings were considered as significant if their absolute values were greater than 0.4. Thus, the classification of factor loadings is “strong,” “moderate,” and “weak,” corresponding to absolute loading values of  $>0.75$ ,  $0.75\text{--}0.50$ , and  $0.50\text{--}0.30$ , respectively (Liu et al., 2003; Pejman et al., 2009). The factor scores for all three isolated factors were saved as new variables, to be used in the construction of multivariate chemographs. It is a bar chart, which on the abscissa shows the cases (water samples with dates) marked according to the clusters previously extracted, and on the ordinate present the factor scores for each factor in a different color. The simplicity of diagram construction and the clear overview of multivariate results in this graphic way provide an advantage over the construction of traditional chemographs for each parameter separately. The novelty of the overall approach is reflected in the common interpretation of the multivariate results, where factor scores were used in the interpretation together with the HCA results to form the conceptual spatio-temporal model of karst hydrogeological system behavior during the flood event.

### 3. Results and Discussion

#### 3.1. Descriptive Statistics

Fourteen physico-chemical variables (EC, pH, T, turbidity, total organic carbon, Ca, Mg, Na, K,  $\text{HCO}_3$ , Cl,  $\text{NO}_3$ ,  $\text{NH}_4$ ,  $\text{SO}_4$ ) and two microbiological variables (total ATP concentration, total bacterial count) were included in the descriptive statistical analyses (Table 1, Figure S1 in Supporting Information S1). As expected, water T from sinking streams (ponor of the Pivka River—PP, ponor of the Rak River—PR) showed pronounced variations (from  $2.3^\circ\text{C}$  to  $12^\circ\text{C}$ ) due to direct contact with the atmosphere, while groundwater showed a similar but slightly dampened pattern of change (from  $4^\circ\text{C}$  to  $11^\circ\text{C}$ ) due to its recharge from sinking streams. The Malenščica spring—SM, which is a diffuse type of spring, showed the lowest coefficients of variation for EC, turbidity, ATP and total bacterial count. The greatest changes were observed at the sampling site PP, which represents a terminal point of the larger surface river network that extends into a valley where human activity is concentrated.

The unique water-type in the studied area is  $\text{Ca-HCO}_3$ , which is common for water in karst regions. Mg was the second abundant cation as the Rak River catchment partially drains areas of dolomitic bedrock (Kogovšek, 2004). The mean values for Na, K, Cl,  $\text{SO}_4$  showed that PP and CP have slightly higher concentrations compared to the other sampling sites, and again this can be explained by the fact that the Pivka River drains areas of flysch bedrock, richer with these elements (Zupan Hajna, 1992).

Conducting descriptive statistical analysis was the first step in selecting parameters for further multivariate statistical analysis. Parameters that showed a low coefficient of variance (e.g., pH) and the parameters that did not show significant variations in concentrations overtime (e.g.,  $\text{NH}_4$ ,  $\text{NO}_3$ , and  $\text{SO}_4$ ) were not considered in further analysis. For further statistical analysis, the parameters EC, Cl, K, turbidity, ATP and bacteria were selected because they showed strong changes over time and/or differences between the studied sites (Table 1). In addition, the Ca/Mg ratio was included as a single variable in the further analysis, as it is a common parameter for meaningful hydrochemical interpretation in karst environments (Fairchild et al., 2000; Moral et al., 2008) and is relevant to the studied area, where sub-catchment C (Figure 1c) is characterized by dolomitic water (Kogovšek, 2004). Considering the high correlation coefficient (Spearman  $r_s$  0.85,  $p < 0.0001$ ) between  $\text{HCO}_3$  and EC, and that  $\text{HCO}_3$  anion is dominant at all sites, EC was included in further analysis, as this parameter contains more information than  $\text{HCO}_3$ . The discharge rate of the springs (Malenščica—SM and Unica—SU) was also additionally included in the further analyses to compare the hydraulic and hydrochemical behavior. Water temperature (T) is not directly included in the multivariate statistical analyses because of additional changes in values due to changes in atmospheric temperature during the flood event. However, T was used as an additional parameter to explain the hydrodynamics of the system.

The intra-site temporal variability of selected physico-chemical parameters is shown in Figure 4. Large variability of parameters occurs in the early period when precipitation began after a long dry period. Thereafter, the values of the observed parameters generally stabilize. The greatest variability at all measurement points is seen in the microbiological parameters. Among the measurement points, the largest variations are characteristic of PP. A



**Table 1**  
*Statistical Characteristics of Hydrochemistry and Microbiology During Sampling Period*

Parameter	EC μS/cm	T °C	pH	Turb NTU	Ca mg/l	Mg mg/l	Na mg/l	K mg/l	HCO <sub>3</sub> mg/l	Cl mg/l	NO <sub>3</sub> mg/l	SO <sub>4</sub> mg/l	NH <sub>4</sub> mg/l	TOC mgC/l	ATP RLU	Bacteria CFU/ml	Q m <sup>3</sup> /s	Ca/Mg meq/l:meq/l	
PP	Min	238	2.3	7.4	1.0	38.7	2.6	2.4	0.4	162	2.5	0.0	3.2	0.0	1.2	79	31	0.13	8.6
	Max	498	12.0	8.0	65.0	82.6	5.2	20.9	4.5	753	27.1	6.1	12.5	0.5	7.8	2,070	2,430	45.9	12
	Mean	363	9.1	7.7	18.1	62.6	3.9	6.8	2.3	297	7.7	3.1	6.2	0.2	4.4	530	787	20.9	9.8
	CV	20.2	23.7	2.2	109	22.1	21.8	71.5	58.9	41.6	93.2	44.4	46.5	63.2	44.9	99	93	70	9.2
PR	Min	355	3.0	7.4	0.5	35.9	7.1	1.2	0.3	249	1.6	1.9	2.4	0.01	1.4	28	19	n.d.	1
	Max	502	11.9	8.1	77.0	75.2	21.7	5.6	2.2	686	9.2	3.5	8.5	1.4	6.4	544	1,240	n.d.	6.2
	Mean	397	8.9	7.7	8.9	64.5	9.8	1.8	0.7	328	2.4	2.6	3.3	0.2	3.2	158	209	n.d.	4.25
	CV	7.7	24.6	2.5	209	13.2	29.3	48.2	57.2	28.5	64.0	18.4	37.4	206	37.4	71	151	n.d.	25
CP	Min	263	6.3	7.3	0.5	43.0	2.6	2.4	0.5	197	1.7	2.4	2.7	0.01	0.9	34	26	n.d.	6.9
	Max	465	11.4	8.0	80.0	82.3	6.3	14.9	3.9	562	19.8	4.9	9.2	1.1	7.3	1,154	1,560	n.d.	12.1
	Mean	378	9.6	7.7	17.4	64.3	4.2	5.9	1.9	295	6.7	3.5	5.3	0.2	3.9	326	478	n.d.	9.5
	CV	14.9	13.8	2.4	120	15.8	20.8	60.2	55.0	27.1	78.6	23.9	36.6	127	43.1	102	109	n.d.	12.8
CR	Min	349	5.0	7.5	0.5	44.7	4.8	1.4	0.2	263	1.6	2.1	2.5	0.0	1.4	4	6	n.d.	4.2
	Max	443	11.1	7.9	26.0	76.6	9.8	10.9	3.5	482	19.9	6.0	9.2	0.6	4.0	502	425	n.d.	8.3
	Mean	399	8.9	7.7	6.5	66.6	7.4	3.1	0.8	315	4.6	3.3	3.8	0.1	2.7	98	101	n.d.	5.6
	CV	5.2	15.6	1.5	126	11.4	19.5	96.1	104	16.6	117	28.5	47.9	113	24.8	109	107	n.d.	18
SU	Min	308	5.5	7.4	0.5	44.7	4.3	1.8	0.3	238	2.0	2.2	2.5	0.0	1.3	27	12	0.51	5.5
	Max	448	11.1	7.9	48.0	75.5	7.7	11.7	2.6	476	19.6	5.1	8.3	1.0	5.8	681	1,880	82.6	8.9
	Mean	386	9.3	7.6	12.5	65.9	6.0	4.7	1.4	309	5.1	3.4	4.4	0.2	3.5	221	410	39	6.8
	CV	9.8	15.0	1.8	106	11.4	18.3	71.3	56.6	20.5	88	24.8	37.9	127	34.8	84	125	67	14.5
SM	Min	373	4.0	7.3	0.5	37.4	5.7	1.3	0.3	274	1.6	2.1	2.2	0.01	1.3	9	5	2.5	3.7
	Max	432	10.5	7.9	8.0	79.8	10.9	3.0	1.2	418	3.9	5.3	4.8	0.9	8.3	259	211	9.1	6.7
	Mean	398	8.8	7.6	2.3	67.8	9.0	1.8	0.6	319	2.3	3.0	3.1	0.2	3.1	66	44	7.4	4.7
	CV	4.1	18.6	2.4	85.3	11.7	16.4	26.2	36.5	11.5	27.3	25.4	23.1	157	46.1	90	107	26.7	17.6

*Note.* Overview of minimum, maximum, mean values, and CV (coefficient of variation) of physicochemical data and discharges (Q): 24 samples for each location, n.d.—no data. PP—ponor of the Pivka River, PR—ponor of the Rak River, CP—Pivka and CR—Rak channels of the Planinska Jama, SU—Unica spring, SM—Malenšiča spring.

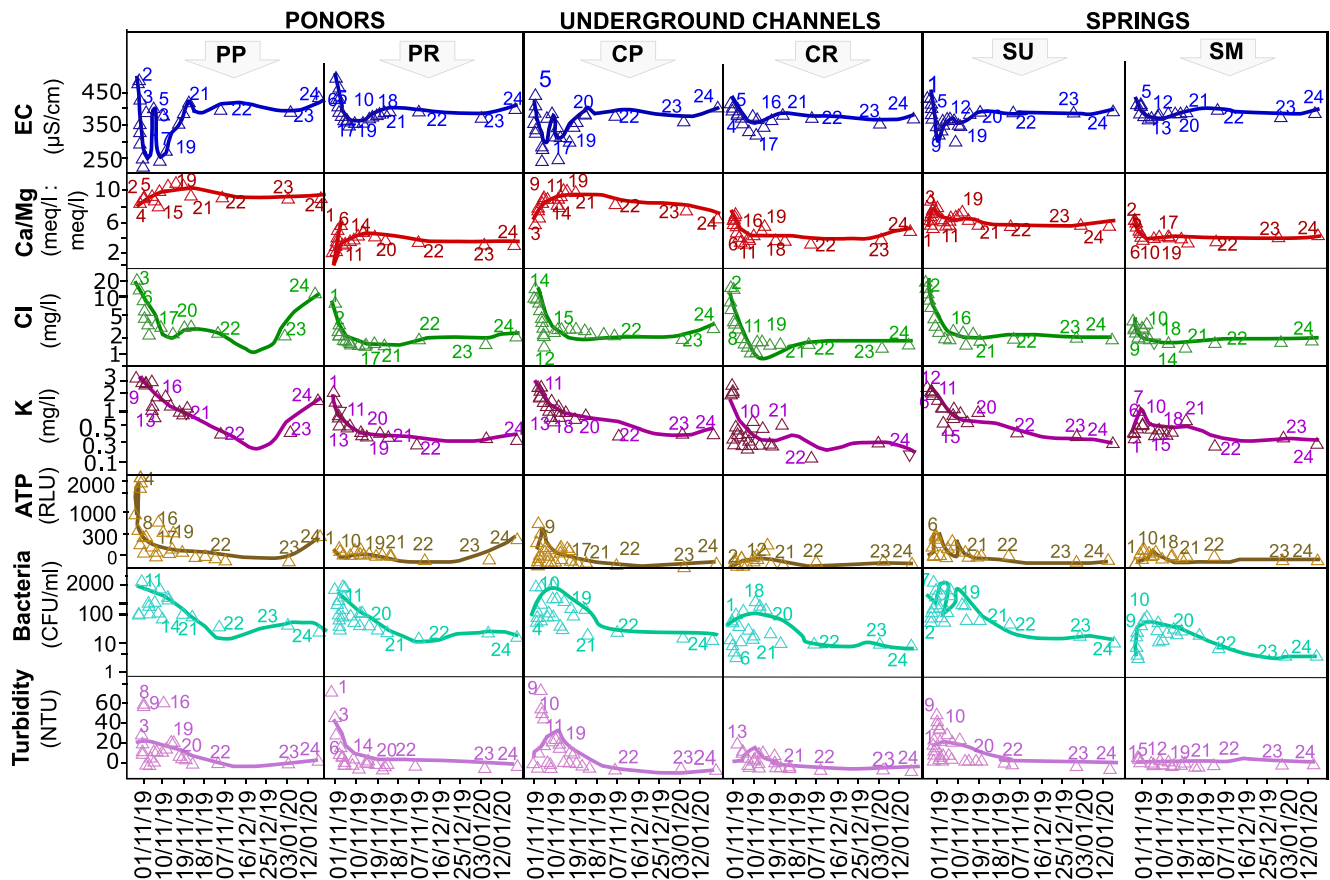


**Figure 4.** Intra-site temporal variability of selected parameters of ponors (PP—ponor of the Pivka River, PR—ponor of the Rak River), underground channels (CP—Pivka channel, CR—Rak channel), and springs (SM—Malenšičica spring, SU—Unica spring). The designation 1–24 means a sequence number of the sample.

similar pattern, appearing in a somewhat attenuated form in CP and then in SU, shows a significant influence of the Pivka River in this part of the karst system. In the rest of the area, the differences are less pronounced, and their interpretation requires further utilization of MST.

### 3.2. Dynamics of Springs Recharge

All selected hydrochemical and microbiological parameters of the springs SM and SU were analyzed with HCA, including the discharges and shown on a two-way heat dendrogram (Figure 5). This type of graphical visualization allows observation of changes in multiple variables in relation to the spring's discharge changes. Distance graph allowed to recognize five temporal phases for each spring. Each phase is characterized by different statistical properties resulting from changes in recharge conditions (C1–C5 in Table 2). Phases were subdivided by visual inspection of two-way heat plot dendrograms (Figure 5). Special attention was paid to grouping the cases and interpreting the influence of each hydrochemical and microbiological variable to identify the strongest influence of the recharge component on each cluster. Only the results of the springs SM and SU are presented here, while the results of the ponors and cave streams are considered as control points and are therefore included in Figures S2–S5 and Text S1–S5 in Supporting Information S1.

At SM (Figure 5a), the cases are grouped in almost the same order in which they were sampled, suggesting gradual changes in the recharge system of this spring. The relation of hydrodynamic and hydrochemical signatures in karst systems has already been highlighted by Hartmann et al. (2013). The discharge ( $Q$ ) shows increasing values, from C1 to C4 (from blue to red field on heat-plot), particularly noticeable in C2, which is reflected also in the increase of EC, K and Cl. In the C3, with a further increase in EC, the most significant increase in bacteria and turbidity is noticeable. As the SM reaches a maximum and stabilization in discharge during phase C4, and decreases slightly after in C5, a dilution of all considered hydrochemical parameters is noticeable. This

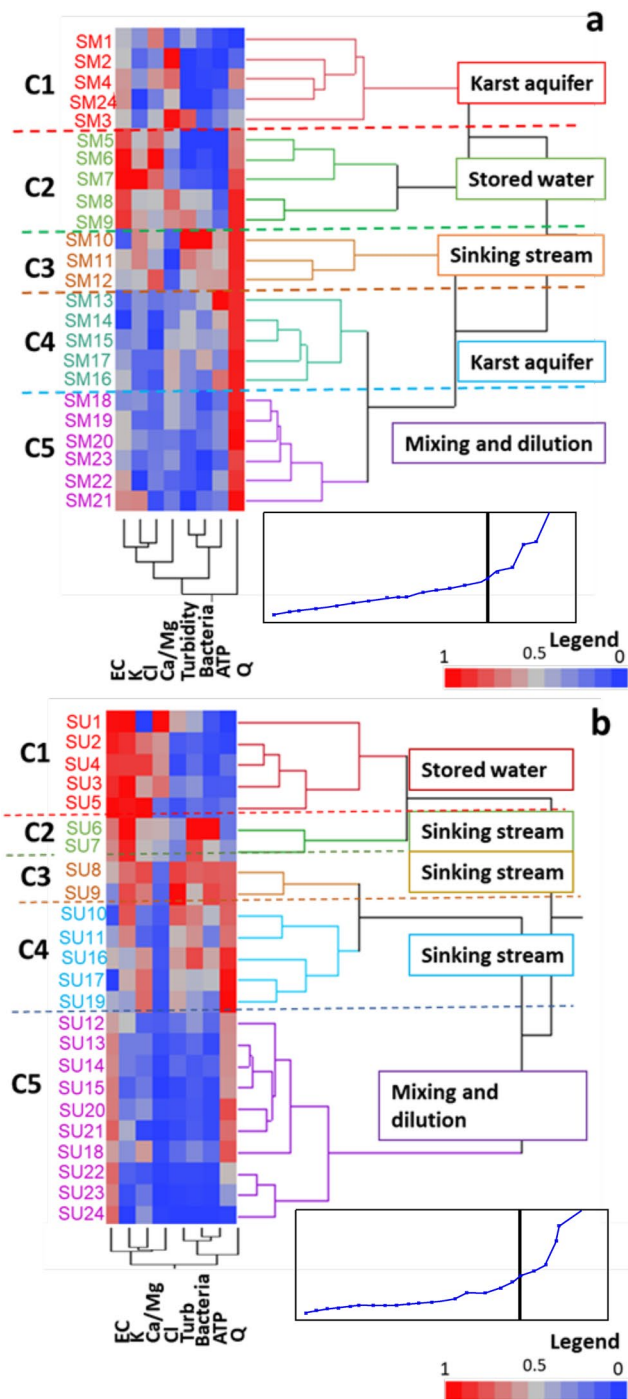


**Figure 5.** Impact of different components of karst hydrological system on observed springs illustrated by two-way dendrogram with heat plot and distance graph (a) SM—Malenščica spring, (b) SU—Unica spring. The color gradient represents the range from the lowest value (blue) to the highest (red) of each variable. SM1–SM24 and SU1–SU24 are labels for collected samples.

relationship can be further confirmed by observing the numbering of the samples in C1 (i.e., SM1–SM4 and SM24). The last sample taken (SM24) shows that the hydrodynamic cycle is completed and the karst system is approaching the initial hydrochemical conditions.

In addition, the first phase C1 is generally characterized by stable low water conditions with higher EC, due to water–rock interaction, but low values of bacteria, ATP and turbidity. Such hydrochemical characteristics resemble the typical recharge from karst aquifer and reflect what is known in the literature as pre-event conditions (Ford & Williams, 2007). The phase represents the starting point for comparison with the values of the other clusters.

The second phase (cluster C2; samples SM5–SM9) is characterized by a significant increase in  $Q$  and EC. Other observed ions (K, Cl, and Mg) increase as well, and there are no significant changes in turbidity and bacteria. Such conditions indicate an outflow of previously stored water from karst channels and unsaturated zone. This is also confirmed by the increase in  $T$  (see Figure S1 in Supporting Information S1) at values characteristic of the karst aquifer (Petrič & Kogovšek, 2010). In contrast, cluster C3 (SM10–SM12) is characterized by a further increase in  $Q$ , but an abrupt increase in bacterial concentration, ATP and turbidity, while EC, Ca/Mg ratio and other observed ions decrease compared to the previous phase C2. The observed microbiological and hydrochemical changes indicate the arrival of low-quality water from sinking streams that are also rich in Mg (Figure S1 in Supporting Information S1). In cluster C4 (SM13–SM17) a decrease in almost all hydrochemical parameters (as well as  $T$  to the values characteristic of karst aquifer) and decrease of ATP level and bacterial concentration (compared to C3) was observed. Since the discharge remains high, the outflow of newly infiltrated water from the karst aquifer system is reflected. The cluster C5 (SM18–SM23) shows similarities with the previous cluster, pointing to the stabilization of conditions in the functioning of the karst aquifer. This is the phase in which water mixing and dilution represent the basic process that affects water quality on the spring.

At SU, two general branches (Figure 5b) connect clusters C1–C2 with the most distant clusters C3–C5. For the first branch, it is characteristic that the samples are in the order of sampling on the dendrogram (SU1–SU7), indicating the gradual changes within the recharge system. The samples on the second branch (C3–C5), which do not follow the sampling order, show the influence of water mixing from different parts of the recharge area and point to a more dynamic recharge system of SU compared to SM.

The first five samples (SU1–SU5) belong to cluster C1, during which  $Q$ , turbidity and microbiological parameters were low, while the values of EC, K and Cl increased. This indicates the discharge of stored water displaced within the conduit. In cluster C2, an increase in  $Q$ , turbidity, ATP and bacterial concentration was observed while EC and some ions like Cl decreased. Also in cluster C3, there was a significant increase in  $Q$ , ATP, turbidity and Ca/Mg ratio, while EC and some ions (K, Cl) decreased. The described characteristics indicate the arrival of water from allogenic recharge. Consequently, it can be assumed that the individual clusters reflect differences in the proportion of recharge from different sub-catchments (Figure S1 in Supporting Information S1). In cluster C4, all observed parameters started to decrease with increasing  $Q$  and significantly lower Ca/Mg ratio. In cluster C5, which contains the largest number of samples, the values of all analyzed parameters decreased significantly, except for EC. This can be explained by the prevailing process of water mixing and dilution.

decrease with increasing  $Q$  and significantly lower Ca/Mg ratio. In cluster C5, which contains the largest number of samples, the values of all analyzed parameters decreased significantly, except for EC. This can be explained by the prevailing process of water mixing and dilution.

**Table 2**  
*Mean Values of Selected Parameters by Clusters for SM—Malenščica Spring and SU—Unica Spring*

	Cluster	Cases	Q m <sup>3</sup> /s	EC μS/cm	Turbidity NTU	K mg/l	Cl mg/l	Ca/Mg	ATP RLU	Bacteria CFU/ml
SM	C1	SM1-SM4, SM24	4.0	396.8	2.0	0.4	2.4	5.6	27	14
	C2	SM5-SM9	7.6	425.0	2.0	0.8	3.0	4.8	20	33
	C3	SM10-SM12	8.5	387.7	5.3	0.7	2.6	3.8	115	138
	C4	SM13-SM17	8.5	383.0	2.4	0.5	1.7	4.6	135	58
	C5	SM18-SM23	8.6	394.5	1.3	0.5	1.9	4.3	54	19
SU	C1	SU1-SU5	6.9	438.2	8	2.4	12	7.6	143	123
	C2	SU6, SU7	16	390.5	11	2.5	8.2	7	609	1,290
	C3	SU8, SU9	58	351	44	1.9	3.9	7.9	380	1,425
	C4	SU10, SU11, SU16, SU17, SU19	69	336.2	24	1.4	3.0	6.9	348	555
	C5	SU12-SU15, SU18, SU20 - SU24	41	390.3	3.4	0.7	2.4	6.1	86	102

### 3.3. Factors Controlling Water Quality Changes

A thorough review of hydraulic behavior and water quality dynamics at all observation points during the flood event was considered in detail using the principal component and FA. The scree-plot of eigenvalues (equal to and greater than 1; Figure 6a) indicated that the first three components provide a trustworthy representation of the data. They represent 79.4% of the total variance in the data set. Bartlett's sphericity test conducted on the data matrix showed that separated components were statistically significant ( $p < 0.0001$ ) to be further evaluated. Interpretation of PCA variable correlation plot (Figure 6b) distinguished three main directions of analyzed parameters, representing three independent processes with different hydrogeochemical indications. The vertices for turbidity, ATP, and bacteria are near equal length and lie close to each other, indicating their proportionality and joint influence. Vertices of Cl, EC, and K generally act in a similar direction, which is orthogonal to the direction of turbidity, ATP, bacteria. The presence of such differences in directions indicates that processes take place independently of each other. PCA isolated the Ca/Mg parameter as the third significant ray, with a less length compared to the previous, indicating the least discriminant power among the examined variables. The direction of Ca/Mg is oriented on the opposite side from one of Cl, indicating their inversely proportional relation.

On the score plot (Figure 6c) the first few samples of almost each sampling location (except SM) are located in the upper right and left quadrant, in the direction of Cl, K, and EC rays. At a somewhat later stage water samples (e.g., samples with numbers 8–10, 16–19) change position and move to the lower right quadrant in the direction of turbidity, ATP, and bacteria, which indicates changes in the recharge properties of the karst system. Grouping of samples from the ponor of the Rak River is noticeable in the direction of action of Ca/Mg ratio rays (lower left quadrant, Figure 6c), corresponding to drainage areas where Upper Triassic dolomites predominate. Tracking of individual samples in the sampling order for springs SM and SU is presented in Figures S6 and S7 in Supporting Information S1. To get into more detail and explain the processes that take place in the study area, FA was performed, and factor loadings were extracted (Table 3). The prevailing factor loadings were considered when the absolute value in the rotated loading matrix was greater than 0.4 (bold in Table 3).

Factor 1 (F1) explained 38% of the variance, and the following variables had the strongest partial contribution: bacteria, turbidity, ATP, while K and EC had moderate and weak contributions, respectively (Table 3). Among these variables, only the EC value had an inverse influence. Bucci et al. (2015) in their 10-year research showed that microorganisms and bacterial cells coupled with other classical tracers are effective to study the recharge and the flow processes in carbonate aquifers. Regarding the quality, besides bacteria, at karst springs the problem is generally correlated with high turbidity during periods of heavy rainfall. Several other studies (e.g., Frank et al., 2018; Mahler et al., 2000; Pronk et al., 2007; Vuilleumier et al., 2021) observed that bacteria are likely to be mobilized together with fine sediments; therefore, large proportions of fecal bacteria in karst aquifers are associated with suspended sediments. In this way, bacteria and turbidity can be considered as important natural tracers in karst systems.

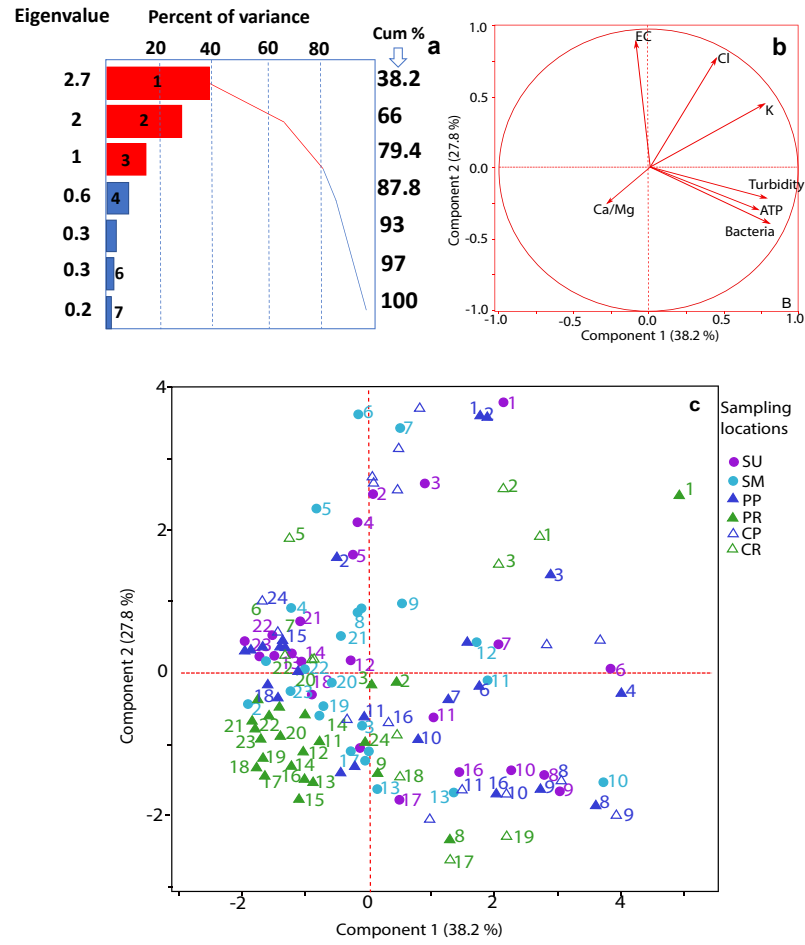


**Figure 6.** (a) Eigenvalues with cumulative percent of variance—red bars indicate eigenvalues equal to and greater than 1, blue bars indicate eigenvalues lower than 1, (b) Variable correlation plot; (c) Projection of cases onto the component-plane (score plot). Ordinal numbers from 1 to 24 indicate locations from each location. Legend of sampling locations: PP—ponor of the Pivka River, PR—ponor of the Rak River), underground channels (CP—Pivka channel, CR—Rak channel), and springs (SM—Malenščica spring, SU—Unica spring).

**Table 3**

Rotated Factor Loadings (Significant Factor Loadings  $\geq 0.4$  Are *Italicized*, While Strong Factor Loadings  $> 0.75$  Are **Bold**)

	F1	F2	F3
Bacteria	<b>0.89</b>	-0.05	-0.01
Turbidity	<b>0.80</b>	0.11	0.01
ATP	<b>0.75</b>	-0.02	-0.15
Cl	0.12	<b>0.91</b>	-0.07
EC	-0.42	<b>0.80</b>	-0.1
K	0.59	0.71	-0.06
Ca/Mg	-0.08	-0.1	<b>0.93</b>
Variance (%)	38	28	13
Factor name	Sinking stream component	Stored water component	Karst aquifer component

Factor 2 (F2) explained 28% of the variance and was dominated by the strong influence of Cl, EC, and the moderate impact of K (Table 3). Their origin in groundwater can be ambiguous. Generally, Cl and K are highly soluble salts considered to be predominantly non-reactive tracers that do not tend to adsorb, transform or decay during transport (Hunkeler & Mudry, 2007; Perrin et al., 2003). They are commonly found in soil. High factor loadings for the observed ions may therefore be associated with the dissolution of salts from the unsaturated zone, that is, soil and epikarst. The presence of increased K and Cl concentrations may also be the result of water interaction with clay minerals in flysch, as these can contain a variable amount of metal ions and alkali metals (Kerr, 1952; Zupan Hajna, 1992). Elevated Cl and K levels (along with NO<sub>3</sub>, SO<sub>4</sub>) may be considered as pollution-related solutes leached during flood events because of agricultural and land-use activities (Dar et al., 2015; Doctor et al., 2006; Mulec et al., 2019; Raeisi et al., 2006). Considering the conservative nature of the strongest components of F2 in this study, namely chloride and EC, the latter also being relatively easy to measure in the field, these two parameters can be considered as significant and reliable natural tracers.

The third factor (F3) is characterized by high positive scores for the Ca/Mg ratio, and it explains 13% of the variance (Table 3). Chemical parameter Ca/Mg ratio may be related to the dissolution processes in karst aquifer, interchanging flows from limestone and dolomite areas, depending on the portion of Mg-calcite and dolomite in parent rocks. On the other hand, the Ca/Mg ratio may reflect the time of interactions between limestone surface and water volume (water residence time) in the unsaturated zone of the aquifer (Celle-Jeanton et al., 2003; Fairchild et al., 2006; Pracný et al., 2017). Although the concentration of Ca and Mg ions may decrease along the flow path of the aquifer in the case of a water-rock interaction, under specific conditions, Mg could be a useful tracer for separating spring conduit flow from the diffuse flow within the karst aquifer (Toran & Reisch, 2013). Considering the lithologically pronounced differences between the contributing sub-catchments in the study area and the fact that the underground flow-paths are characterized by well-developed channels in which the transport is relatively fast, it can be assumed that there were no significant changes in the concentration due to the aforementioned hydrogeochemical processes. Given that the ratio Ca/Mg was the only significant for F3, it is considered as important parameter for identification of the karst aquifer component and interchanging flows from limestone and dolomite areas.

The three isolated factors can be interpreted as follows: F1 is a component of the hydrologic system associated with bacteria, increased turbidity, and low EC suggesting the arrival of allochthonous water, named as the "sinking stream component." F2 is a component that leads to increased EC, particularly contents of Cl and K, that originate from riverbed rinsing or the soil/unsaturated zone, named as the "stored water component" either in karst or non-karst environment. F3 is a component representing a karst aquifer impact, labeled as the "karst aquifer component." The third factor is influenced by the Ca/Mg ratio, so that the inversely proportional effect of this factor can again be interpreted as an inflow of groundwater with elevated Mg concentrations from recharge areas in the dolomite.

### 3.4. Multivariate Chemographs

Multivariate chemographs were constructed to provide an overview of the various influences and processes in the karst aquifer system (Figure 7). The simultaneous evaluation of the influence of the factors on the isolated clusters allowed a more detailed representation of the predominant processes and the duration of the dynamic phases of the observed event. The influence of all three isolated factors is clearly visible for each sampling point within the associated hydrodynamic phase. Each cluster was named according to the predominant influence of each component. When F1 and F2 were both high, we considered the phase to be under the influence of "stagnant water".

The shapes of the multivariate chemographs and the distribution of factor scores for PP, CP, and partially SU (Figures 7a, 7c, and 7e) show great similarities, confirming a direct hydraulic connection between these points. Changes that occur at PP are reflected in the other points with a 1-day delay. When looking at the plots for PR and CR (Figures 7b and 7d), the similarities in shapes are not as clear, indicating the possibility of additional water inflow or various hydrochemical and microbiological processes in the channel flow, including mixing of water.

From the shape of the diagram for the springs (Figures 7e and 7f), it can be seen that the time series of hydrochemical and microbiological tracers and the quantitative responses of the springs to precipitation are different, indicating diverse dynamics of the hydrogeological systems of the two springs. The basic characteristic of SM is

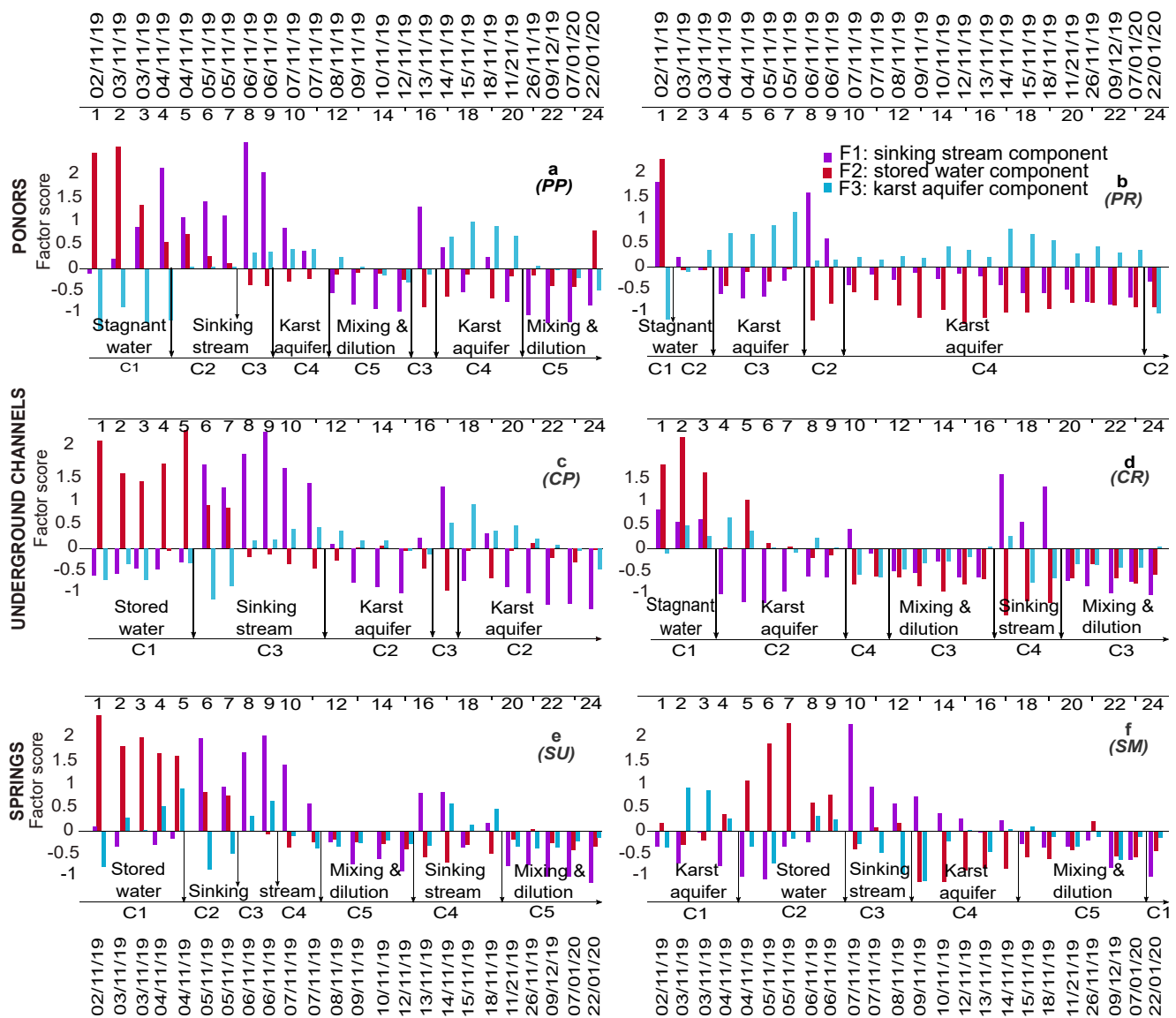


**Figure 7.** Multivariate chemographs of each sampling location: (a) PP—ponor of the Pivka River (b) PR—ponor of the Rak River, (c) CP—Pivka channel, (d) CR—Rak channel, (e) SU—Unica spring, (f) SM—Malenščica spring. The numbers 1–24 indicate the serial number of the samples.

that there were no significant hydrochemical or microbiological changes even a few days after the precipitation event (Figure 7f; C1). Moreover, only at SM is the karst aquifer component (F3) dominant in the initial phase (C1); at all other sites, the dominant factor in the initial phase is F2, indicating the presence of stored or stagnant water. In the next phase, the discharge of stored water begins (influence of factor F2 on cluster C2). On 7 November sudden changes occur and the spring begins to reflect the influence of sinking rivers (impact of F1 on C3). As this influence subsides, an increased proportion of recharge from the karst aquifer and stabilization of the chemical and microbiological composition of the karst water are observed (increase of F3; C4). In the last phase (C5), dilution of all waters is observed, with all three factors having a predominantly negative effect.

The first period at SU lasts 2 days (Figure 7e; C1), during which this spring discharges previously stored water (F2). Thereafter, the influence of the sinking streams predominates in the period after 5 November (C2–C4), which is marked by the strong influence of F1. On 8 November, the intense rains cease and the water is mainly diluted (C5). Again after a new rainfall, between 15 and 18 November, the distribution of factor scores on the multivariate chemograph is similar to PP and CP sites. Finally, water dilution occurs and all three factors have a negative influence, leading to a stabilization of hydrochemical and microbiological parameters (C5).

### 3.5. Spatio-Temporal Conceptual Model of the Karst System Hydrodynamics

The results of the MST and the multivariate chemographs were utilized to develop a spatio-temporal conceptual model of a complex karst system behavior. The matrix system is mostly comprised of matrix pores and microfractures, which play a role in higher water storage and flow following Darcy's law. On contrary, the conduit system is often characterized by fast and turbulent flow (Wu & Hunkeler, 2017; Zhao et al., 2022). The duality of hydraulic properties causes temporal hydrologic variability and gradient reversal in the aquifer. During low water, the karst conduit system has a low water level and causes the water surrounding the matrix to flow into the conduit, while at high water, the increase in hydraulic pressure in the conduits and the rise in water level causes water from the conduits to penetrate the matrix volumes. These general assumptions were used in considering the functioning of the karst hydrogeological system (KHS) on the basis of which the general groundwater levels have been established and schematized.

Under the monitored hydrological conditions, significant changes in the measured parameters were observed during the initial phase of the flood event. During this period, water quality decreased the most. Thereafter, differences between sites were much less significant. Therefore, four flow regimes were considered important for the study of hydrodynamics and transport of contaminants including (a) low water conditions in KHS—initial increase in discharge after the precipitation event, (b) medium water conditions in KHS—significant increase in discharge, (c) high water conditions in KHS—first peak in discharge, (d) high water conditions in KHS—discharge slightly decreasing. In the conceptual model, individual elements are schematized and highlighted to focus on the main hydrodynamic processes in the KHS (this mainly refers to the representation of groundwater, the filling of the channels with water and the ponor zones; Figure 8).

The main identified water components that recharge KHS (sinking stream, karst aquifer, stored and stagnant water) and associated processes (mixing and dilution) identified with HCA were included in the model. Based on PCA and FA, parameters with strong factor loadings ( $>0.75$ ) were selected and also included: F1—sinking stream component with bacteria and turbidity; F2—stored water component with EC and Cl; F3—karst aquifer component with Ca/Mg ratio.

After a dry period, a rain event on 2 November triggered the beginning of the rise in the general water table in KHS. The stagnant water at the ponors (left small sketch on Figure 8a) had its highest EC value and increased values of ATP, which reflected total microbial biomass including live and dead microbes (PR and PP with a positive influence of F2 and F1). At CP, the influence of stored water dominated (+F2; right small sketch on Figure 8a). At CR, stagnant water was retained in the channel (+F1, +F2).

Meanwhile there was a marked increase in the discharge at the springs. At SU the previously stored water was discharging, with the highest EC (+F2). At SM the situation was different, the predominant role of the karst aquifer component (+F3) indicated the prevailing influence of autogenous recharge (from sub-catchment B). This was also indicated by the differences in water temperature between SM and CR (consistently around 8.9°C at SM and from 9.5 to 11°C at CR). The influence had previously been demonstrated by a tracer test (Michler, 1955) and by numerical modeling (Kaufmann et al., 2020), which showed that under low hydrological conditions, water from a syphon deep in the CR cave system flows through unknown pathways toward SM rather than through the known galleries of CR toward SU.

In the next phase (Figure 8b), the process of intensive flushing of the riverbed gradually prevailed at PP with increasing values of turbidity and bacteria (+F1, +F2). The influence was noticeable on CP as well as on SU where maximum bacteria count (1,880 CFU/ml) was reached with 1-day delay. At PR the initial conditions changed abruptly (left small sketch in Figure 8b) and were influenced by the karst aquifer component from the sub-catchment B (+F3, -F1). CR in addition to the karst component discharged also stored water (+F3, -F1, +F2). Due to the gradual rise of the general water level in the KHS and the hydraulic interaction between the karst conduits and the adjacent rock matrix, water penetrated the entire hierarchy of pores and openings. The partitioned zones were reconnected through the annexes of the drainage system and a continuous flow through all types of hydraulically connected openings was established (Mangin, 1975). The stored water (+F2) started to transfer from distant parts of the system (right small sketch in Figure 8b). For this reason and/or because of the catchment extension stored water was discharging also at SM, characterized by the highest EC values for this spring (+F2). In this phase, the complexity of the KHS and interconnections of the karst channels were particularly highlighted.



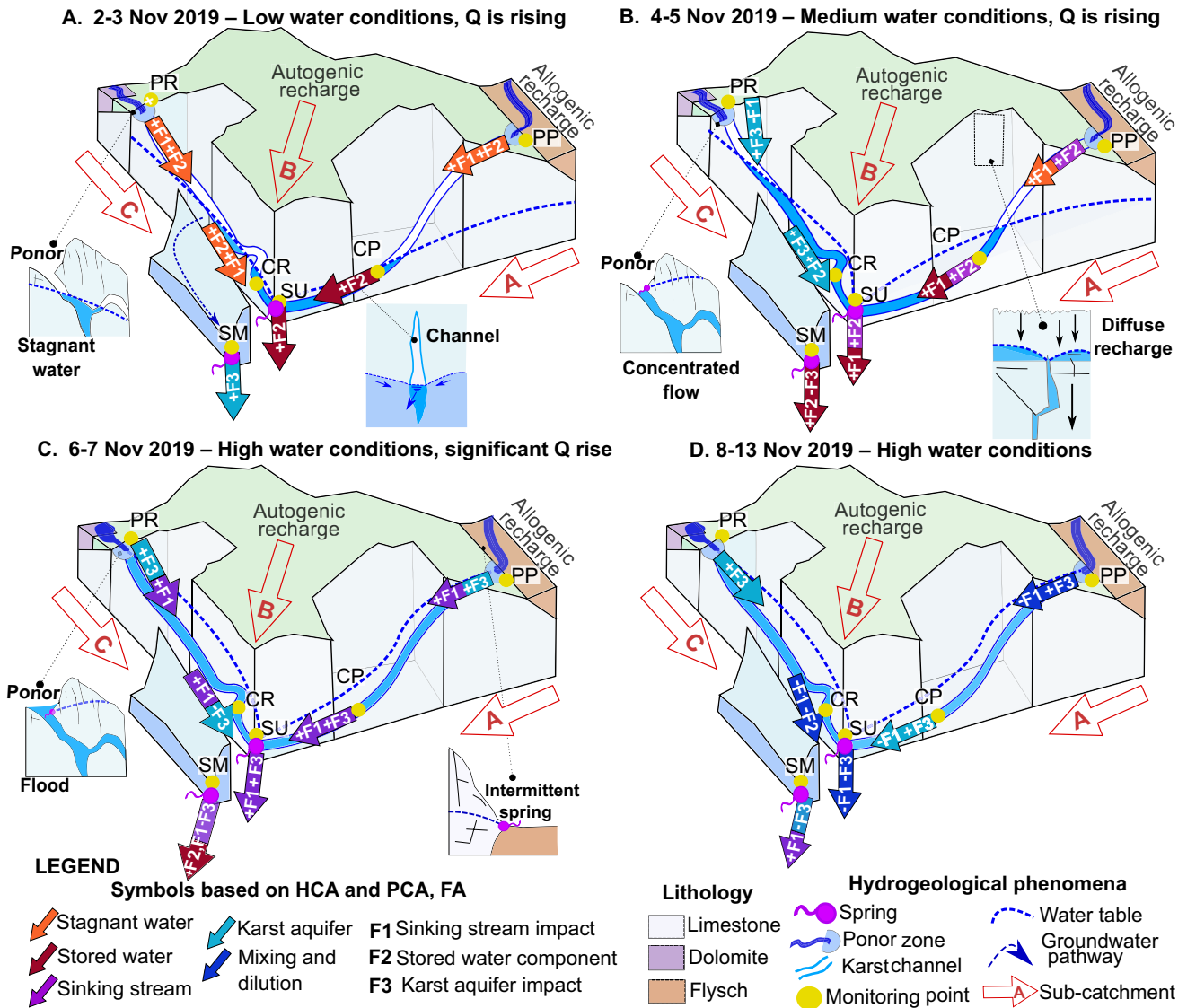


**Figure 8.** Conceptual spatio-temporal model of a complex karst system with characteristic recharge directions defined on the basis of principal components that is, natural tracers. General groundwater levels are schematized. Monitoring points: PP—ponor of the Pivka River, PR—ponor of the Rak River, CP—Pivka channel, CR—Rak channel, SM—Malenščica spring, SU—Unica spring.

After additional rain, the general water table increased significantly on 6 November at all monitoring points leading to flooding conditions in the KHS (Figure 8c). Water coming from the ponors carried the largest amount of bacterial contamination (PP: 2,430 CFU/ml, PR: 1,240 CFU/ml; highest F1). Within a delay of one or 2 days bacterial contamination occurred in the cave channels and springs (+F1). The increase of the general water table in KHS lead to the appearance of intermittent karst springs in the base of the sub-catchment B and additionally recharged PP (+F3; right small sketch on Figure 8c).

Since the sinking stream of sub-catchment C is recharged also from the dolomitic part, the negative influence of F3 was in this phase characteristic for CR and SM (low Ca/Mg ratio). Due to the well-structured hydrogeological system of the SM catchment, the transfer of water pressure in the system was relatively slow, and the effects of the sinking stream occurred with a delay. On the other hand, SU was thus under the influence of both the sinking streams (+F1) and the karst aquifer (+F3).

In the last phase, the general water tables slightly declined and high-water conditions still prevailed in KHS. The processes of water mixing and dilution predominated at PP and only a slight positive influence of F3 showed

that the proportion of karst water was significant. This condition was also reflected at CP. The processes of water mixing and dilution were more pronounced at SU, resulting in hydrochemical and microbiological stabilization after the end of the influence of F1. At PR, the influence of karst water from sub-catchment B was also significant (+F3). At CR and SM, the influence of the previously prevailing sinking stream from sub-catchment C decreased (decrease of F1), and the negative effects of F2 and F3 announced water dilution and stabilization processes of the chemical and microbiological composition of the water.

#### 4. Conclusions

Multivariate statistical techniques are excellent tools for determining the dynamics of recharge mechanisms in karst aquifers, especially when complex systems are involved. However, in more hydrochemically homogeneous environments, they are less efficient in achieving a better understanding. Therefore, in this study, an improved analytical method was developed and applied to interpret water quality dynamics in an integral groundwater flow system. The case study of the binary karst system in SW Slovenia with good hydrogeological knowledge shows that the applied approach improves the understanding of the hydrodynamics of karst groundwater under flood events. Basic underground flow connections in the system ponor-cave-spring were already known based on previous researches (e.g., tracer test, basic comparisons of physico-chemical data). However, only the use of an improved analytical approach allowed a more precise spatiotemporal breakdown of the individual phases in the process of recharge of the two karst springs.

Based on the monitoring of hydrochemical and microbiological indicators as natural tracers, the combined application of HCA, PCA and FA allowed the construction of multivariate chemographs. HCA enabled determination of different phases of springs recharge, each defined in hydrodynamic and hydrochemical terms. In addition, PCA and FA were used to define the predominant factors and principal components of recharge: (F1) the sinking stream component with bacteria and turbidity as main parameters, (F2) the stored water component with EC and Cl as main parameters, and (F3) the karst aquifer component with Ca/Mg ratio as the main parameter. In addition to the observation of springs, access to ponors and water caves provided further insight and a holistic spatial observation of the functioning of the hydrological system. The overall methodology was crucial for the development of an appropriate spatio-temporal conceptual model of the system behavior during the flood event, the definition of the recharge areas, and the main hydrological processes.

The study has shown that the responses of the springs studied are characterized by the different recharge dynamics of the hydrogeological sub-catchments that determine their behavior. Their water quality is most variable during the first more intense precipitation after a long dry period. The results obtained can be used to optimize future water quality parameters for detailed monitoring of dynamic phases.

#### Data Availability Statement

The open repository for downloading the data sets obtained and used in this study is available at <https://metadata.izrk.zrc-sazu.si/srv/api/records/e94359d4-ea34-450b-a28c-4ed83a59b6c5>. Data from the ARSO Hydrological data archive, Ministry of the Environment and Spatial Planning, Slovenian Environment Agency, Available online: <http://www.arso.gov.si/vode/podatki/> (accessed on 23 June 2020), and <http://meteo.arso.gov.si/met/sl/archive/> (accessed on 14 January 2021) were used in the creation of this manuscript. Maps were created using ArcGIS version 10.7 (ESRI, 2011. ArcGIS Desktop: Release 10. Redlands, CA: Environmental Systems Research Institute) available under the ESRI license at <https://www.esri.com/en-us/arcgis/products/arcgis-desktop/buy>. Graphical processing of figures was performed using software Inkscape version 0.92.4 (The Inkscape Project, 2019), available at <https://inkscape.org/release/inkscape-0.92.4/>. Preparation of manuscript, statistical data analysis and preparation of figures were done using Microsoft 365 Apps for enterprise, available at <https://www.microsoft.com/en-ww/microsoft-365/compare-microsoft-365-enterprise-plans?market=af>.

#### References

- ARSO. (2020). Ministry of the Environment and Spatial Planning, Slovenian Environment Agency, hydrological data archive. Retrieved from <http://www.arso.gov.si/vode/podatki/>
- ARSO. (2021). Ministry of the Environment and Spatial Planning, Slovenian Environment Agency, precipitation data archive. Retrieved from <http://meteo.arso.gov.si/met/sl/archive/>

#### Acknowledgments

This study was conducted within the context of the Characterization of karst aquifers on regional and local scales: the recharge area of the Malni water source, No. L7-2630, Infiltration processes in forested karst aquifers under changing environment, J2-1743, Ecohydrological study of spatio-temporal dynamics in karst critical zones under different climate conditions, No. NK-0002, and the programme Karst Research, No. P6-0119, all financially supported by the Slovenian Research Agency (ARRS). The study is also a product of the bilateral cooperation BI-RS/18-19-027 supported by ARRS and Ministry of Education, Science and Technological Development of the Republic of Serbia (2018–2019/Record no. of bilateral project: 28). The authors also acknowledge the help of the laboratory technician Sara Skok.

- Bakalowicz, M. (2005). Karst groundwater: A challenge for new resources. *Hydrogeology Journal*, 13(1), 148–160. <https://doi.org/10.1007/s10040-004-0402-9>
- Barbel-Périneau, A., Barbiero, L., Danquigny, C., Emblanch, C., Mazzilli, N., Babic, M., et al. (2019). Karst flow processes explored through analysis of long-term unsaturated-zone discharge hydrochemistry: A 10-year study in Rustrel, France. *Hydrogeology Journal*, 27(5), 1711–1723. <https://doi.org/10.1007/s10040-019-01965-6>
- Barberá, J. A., & Andreo, B. (2012). Functioning of a karst aquifer from S Spain under highly variable climate conditions, deduced from hydrochemical records. *Environmental Earth Sciences*, 65(8), 2337–2349. <https://doi.org/10.1007/s12665-011-1382-4>
- Bartlett, M. S. (1954). A note on the multiplying factors for various Chi Square approximations. *Journal of the Royal Statistical Society: Series B*, 16(2), 296–298. <https://doi.org/10.1111/j.2517-6161.1954.tb00174.x>
- Benhamiche, N., Sahi, L., Tahar, S., Bir, H., Madani, K., & Laignel, B. (2016). Spatial and temporal variability of groundwater quality of an Algerian aquifer: The case of Soummam Wadi. *Hydrological Sciences Journal*, 61(4), 775–792. <https://doi.org/10.1080/02626667.2014.966723>
- Bicalho, C., Batiot-Guilhe, C., Seidel, J., Van-Exter, S., & Jourde, H. (2010). Investigation of groundwater dynamics in a Mediterranean Karst system by using multiple hydrogeochemical tracers. In: In B. Andreo, F. Carrasco, J. Durán, & J. LaMoreaux (Eds.), *Advances in research in karst media*. *Environmental Earth Sciences*. Springer. [https://doi.org/10.1007/978-3-642-12486-0\\_2](https://doi.org/10.1007/978-3-642-12486-0_2)
- Bicalho, C. C. (2010). Hydrochemical characterization of transfers in karst aquifers by natural and anthropogenic tracers. Example of a Mediterranean karst system, the Lez karst aquifer (Southern France). Hydrology. (ffNNT: 2010AGPT0082ff. ffpastel-00569544f, NNT: 2010AGPT0082) AgroParisTech.
- Brown, C. E. (1998). *Applied multivariate statistics in geohydrology and related sciences*. Springer.
- Bucci, A., Petrella, E., Naclerio, G., Allocca, V., & Celico, F. (2015). Microorganisms as contaminants and natural tracers: A 10-year research in some carbonate aquifers (southern Italy). *Environmental Earth Sciences*, 74(1), 173–184. <https://doi.org/10.1007/s12665-015-4043-1>
- Celle-Jeanton, H., Emblanch, C., Mudry, J., & Charmoille, A. (2003). Contribution of time tracers ( $Mg^{2+}$ , TOC,  $\delta^{13}C_{TDIC}$ ,  $NO_3^-$ ) to understand the role of the unsaturated zone: A case study—Karst aquifers in the doubs valley, eastern France. *Geophysical Research Letters*, 30(6). <https://doi.org/10.1029/2002GL016781>
- Chang, W., Wan, J., Tan, J., Wang, Z., Jiang, C., & Huang, K. (2021). Responses of spring discharge to different rainfall events for single-Conduit Karst aquifers in Western Hunan province, China. *International Journal of Environmental Research and Public Health*, 18(11), 5775. <https://doi.org/10.3390/ijerph18115775>
- Culver, D. C., & Pipan, T. (2013). Subterranean ecosystems. In S. A. Levin (Ed.), *Encyclopedia of biodiversity* (2nd ed., pp. 49–62). Academic Press.
- Dar, F. A., Perrin, J., Ahmed, S., Narayana, A. C., & Riotte, J. (2015). Hydrogeochemical characteristics of Karst Aquifer from a semi-arid region of Southern India and impact of rainfall recharge on groundwater chemistry. *Arabian Journal of Geosciences*, 8(5), 2739–2750. <https://doi.org/10.1007/s12517-014-1440-9>
- Davis, J. C. (1973). *Statistics and data analysis in Geology*. Wiley.
- Demlie, M., Wöhrlich, S., Wisotzky, F., & Gizaw, B. (2007). Groundwater recharge, flow and hydrogeochemical evolution in a complex volcanic aquifer system, central Ethiopia. *Hydrogeology Journal*, 15(6), 1169–1181. <https://doi.org/10.1007/s10040-007-0163-3>
- Doctor, D. H., Calvin Alexander, E., Jr., Petrič, M., Kogovšek, J., Urbanc, J., Lojen, S., & Stichler, W. (2006). Quantification of karst aquifer discharge components during storm events through end-member mixing analysis using natural chemistry and stable isotopes as tracers. *Hydrogeology Journal*, 14(7), 1171–1191. <https://doi.org/10.1007/s10040-006-0031-6>
- Fairchild, I. J., Borsato, A., Tooth, A. F., Frisia, S., Hawkesworth, C. J., Huang, Y. M., et al. (2000). Controls on trace element (Sr–Mg) compositions of carbonate cave waters: Implications for speleothem climatic records. *Chemical Geology*, 166(3–4), 255–269. [https://doi.org/10.1016/S0009-2541\(99\)00216-8](https://doi.org/10.1016/S0009-2541(99)00216-8)
- Fairchild, I. J., Smith, C. L., Baker, A., Fuller, L., Spötl, C., Matthey, D., et al. (2006). Modification and preservation of environmental signals in speleothems. *Earth-Science Reviews*, 75(1–4), 105–153. <https://doi.org/10.1016/j.earscirev.2005.08.003>
- Ford, D., & Williams, P. (2007). *Karst hydrogeology and geomorphology*. Wiley.
- Fournier, M., Massei, N., Bakalowicz, M., Dussart-Baptista, L., Rodet, J., & Dupont, J. P. (2007). Using turbidity dynamics and geochemical variability as a tool for understanding the behavior and vulnerability of a karst aquifer. *Hydrogeology Journal*, 15(4), 689–704. <https://doi.org/10.1007/s10040-006-0116-2>
- Frank, S., Goepfert, N., & Goldscheider, N. (2018). Fluorescence-based multi-parameter approach to characterize dynamics of organic carbon, faecal bacteria and particles at alpine karst springs. *Science of the Total Environment*, 615, 1446–1459. <https://doi.org/10.1016/j.scitotenv.2017.09.095>
- Gabrovšek, F., Kogovšek, J., Kovačič, G., Petrič, M., Ravbar, N., & Turk, J. (2010). Recent results of tracer tests in the catchment of the Unica River (SW Slovenia). *Acta Carsologica*, 39/1(1), 27–37. <https://doi.org/10.3986/ac.v39i1.110>
- Gao, Z., Liu, J., Xu, X., Wang, Q., Wang, M., Feng, J., & Fu, T. (2020). Temporal variations of spring water in Karst areas: A case study of Jinan spring area, northern China. *Water*, 12(4), 1009. <https://doi.org/10.3390/w12041009>
- Giese, M., Reimann, T., Bailly-Comte, V., Maréchal, J. C., Sauter, M., & Geyer, T. (2018). Turbulent and laminar flow in karst conduits under unsteady flow conditions: Interpretation of pumping tests by discrete conduit-continuum modeling. *Water Resources Research*, 54(3), 1918–1933. <https://doi.org/10.1002/2017WR020658>
- Goldscheider, N. (2015). Overview of methods applied in Karst hydrogeology. In Z. Stevanović (Ed.), *Karst aquifers—characterization and Engineering*. *Professional Practice in Earth Sciences*. Springer. [https://doi.org/10.1007/978-3-319-12850-4\\_4](https://doi.org/10.1007/978-3-319-12850-4_4)
- Güler, C., Thyne, G. D., McCray, J. E., & Turner, A. K. (2002). Evaluation of graphical and multivariate statistical methods for classification of water chemistry data. *Hydrogeology Journal*, 10(4), 455–474. <https://doi.org/10.1007/s10040-002-0196-6>
- Hartmann, A., Weiler, M., Wagener, T., Lange, J., Kralik, M., Humer, F., et al. (2013). Process-based karst modelling to relate hydrodynamic and hydrochemical characteristics to system properties. *Hydrology and Earth System Sciences*, 17(8), 3305–3321. <https://doi.org/10.5194/hess-17-3305-2013>
- Holland, S. M. (2006). *Cluster Analysis*. University of Georgia, Department of Geology.
- Hunkeler, D., & Mudry, J. (2007). Hydrochemical methods. Methods in Karst hydrogeology. In N. Goldscheider & D. Drew (Eds.), *International Contributions to Hydrogeology* (Vol. 26, pp. 93–121). Taylor & Francis.
- Inkscape Project. (2019). Inkscape. Retrieved from <https://inkscape.org>
- Jemcov, I., & Čuk Đurović, M. (2020). A hydraulic–hydrochemical approach to impact assessment of a grout curtain on karst aquifer behavior. *Hydrogeology Journal*, 29(1), 179–197. <https://doi.org/10.1007/s10040-020-02245-4>
- Jiang, Y., Wu, Y., Groves, C., Yuan, D., & Kambesis, P. (2009). Natural and anthropogenic factors affecting the groundwater quality in the Nandong karst underground system in Yunan, China. *Journal of Contaminant Hydrology*, 109(1–4), 49–61. <https://doi.org/10.1016/j.jconhyd.2009.08.001>

- Kaiser, H. F. (1960). The application of electronic computers to factor analysis. *Educational and Psychological Measurement*, 20(1), 141–151. <https://doi.org/10.1177/001316446002000116>
- Kaufmann, G., Mayaud, C., Kogovšek, B., & Gabrovšek, F. (2020). Understanding the temporal variation of flow direction in a complex karst system (Planinska Jama, Slovenia). *Acta Carsologica*, 49(2–3), 213–228. <https://doi.org/10.3986/ac.v49i2-3.7373>
- Kerr, P. F. (1952). Formation and occurrence of clay minerals. *Clays, Clay Mineral*, 1, 19–32. <https://doi.org/10.1346/CCMN.1952.0010104>
- Kogovšek, J. (2004). Fizikalno-kemične značilnosti voda v zaledju Malenščice (Slovenija). *Acta Carsologica*, 33(1), 143–158. <https://doi.org/10.3986/ac.v33i1.321>
- Kovács, A., Perrochet, P., Király, L., & Jeannin, P.-Y. (2005). A quantitative method for the characterisation of karst aquifers based on spring hydrograph analysis. *Journal of Hydrology*, 303(1–4), 152–164. <https://doi.org/10.1016/j.jhydrol.2004.08.023>
- Li, P., Tian, R., & Liu, R. (2019). Solute Geochemistry and multivariate analysis of water quality in the Guohua phosphorite mine, Guizhou province, China. *Exposure and Health*, 11(2), 81–94. <https://doi.org/10.1007/s12403-018-0277-y>
- Liu, C. W., Lin, K. H., & Kuo, Y. M. (2003). Application of factor analysis in the assessment of groundwater quality in a Blackfoot disease area in Taiwan. *Science of the Total Environment*, 313(1–3), 77–89. [https://doi.org/10.1016/S0048-9697\(02\)00683-6](https://doi.org/10.1016/S0048-9697(02)00683-6)
- Mahler, B. J., Personne, J. C., Lods, G. F., & Drogue, C. (2000). Transport of free and particulate-associated bacteria in karst. *Journal of Hydrology*, 238(3–4), 179–193. [https://doi.org/10.1016/S0022-1694\(00\)00324-3](https://doi.org/10.1016/S0022-1694(00)00324-3)
- Mangin, A. (1975). Contribution à l'étude hydrodynamique des aquifères karstiques. *Annales de Speleologie*, 26, 283–339.
- Massart, D. L., & Kaufman, L. (1983). *The interpretation of analytical chemical data by the Use of cluster Analysis*. Wiley.
- Michler, I. (1955). Rakov rokav Planinske jame. *Acta Carsologica*, 1, 73–90.
- Moore, P. J., Martin, J. B., & Sreaton, E. J. (2009). Geochemical and statistical evidence of recharge, mixing, and controls on spring discharge in an eugenic karst aquifer. *Journal of Hydrology*, 376(3–4), 443–455. <https://doi.org/10.1016/j.jhydrol.2009.07.052>
- Moral, F., Cruz-Sanjulian, J. J., & Olias, M. (2008). Geochemical evolution of groundwater in the carbonate aquifers of Sierra de Segura (Betic Cordillera, southern Spain). *Journal of Hydrology*, 360(1–4), 281–296. <https://doi.org/10.1016/j.jhydrol.2008.07.012>
- Mudarra, M., & Andreo, B. (2011). Relative importance of the saturated and the unsaturated zones in the hydrogeological functioning of karst aquifers: The case of Alta Cadena (Southern Spain). *Journal of Hydrology*, 397(3–4), 263–280. <https://doi.org/10.1016/j.jhydrol.2010.12.005>
- Mudarra, M., Andreo, B., Barberá, J. A., & Mudry, J. (2014). Hydrochemical dynamics of TOC and NO<sub>3</sub>—contents as natural tracers of infiltration in karst aquifers. *Environmental Earth Sciences*, 71(2), 507–523. <https://doi.org/10.1007/s12665-013-2593-7>
- Mulec, J., Petrič, M., Koželj, A., Brun, C., Batagelj, E., Hladnik, A., & Holko, L. (2019). A multiparameter analysis of environmental gradients related to hydrological conditions in a binary karst system (underground course of the Pivka River, Slovenia). *Acta Carsologica*, 48(3). <https://doi.org/10.3986/ac.v48i3.7145>
- Neilson, B. T., Tennant, H., Stout, T. L., Miller, M. P., Gabor, R. S., Jameel, Y., et al. (2018). Stream centric methods for determining groundwater contributions in karst mountain watersheds. *Water Resources Research*, 54(9), 6708–6724. <https://doi.org/10.1029/2018WR022664>
- Page, R. M., Besmer, M. D., Epting, J., Sigrist, J. A., Hammes, F., & Huggenberger, P. (2017). Deeper insights into water quality dynamics in spring water. *Science of the Total Environment*, 599–600, 227–236. <https://doi.org/10.1016/j.scitotenv.2017.04.204>
- Pejman, A. H., Nabi Bidhendi, G. R., Karbassi, A. R., Mehrdadi, N., & EsmaeiliBidhendi, M. (2009). Evaluation of spatial and seasonal variations in surface water quality using multivariate statistical techniques. *International Journal of Environmental Science and Technology*, 6(3), 467–476. <https://doi.org/10.1007/BF03326086>
- Perrin, J. (2003). *A conceptual model of flow and transport in a karst aquifer based on spatial and temporal variations of natural tracers (Ph.D. thesis)*. Faculty of Sciences of the University of Neuchâtel.
- Perrin, J., Jeannin, P. Y., & Zwahlen, F. (2003). Epikarst storage in a karst aquifer: A conceptual model based on isotopic data, Milandre test site, Switzerland. *Journal of Hydrology*, 279(1–4), 106–124. [https://doi.org/10.1016/S0022-1694\(03\)00171-9](https://doi.org/10.1016/S0022-1694(03)00171-9)
- Petrič, M. (2010). Case Study: Characterization, exploitation, and protection of the Malenščica karst spring, Slovenia. In N. Krešič & Z. Stevanović (Eds.), *Groundwater Hydrology of springs* (pp. 428–441). Butterworth-Heinemann. <https://doi.org/10.1016/B978-1-85617-502-9.00021-9>
- Petrič, M., & Kogovšek, J. (2010). Water temperature as a natural tracer—a case study of the Malenščica karst spring (SW Slovenia). *Geologia Croatica*, 63(2), 171–177. <https://doi.org/10.4154/gc.2010.14>
- Pracný, P., Faimon, J., Všíanský, D., & Kabelka, L. (2017). Evolution of Mg/Ca ratios during limestone dissolution under epikarstic conditions. *Aquatic Geochemistry*, 23(2), 119–139. <https://doi.org/10.1007/s10498-017-9313-y>
- Pronk, M., Goldscheider, N., & Zopf, J. (2009). Microbial communities in karst groundwater and their potential use for biomonitoring. *Hydrogeology Journal*, 17(1), 37–48. <https://doi.org/10.1007/s10040-008-0350-x>
- Pronk, M., Goldscheider, N., & Zopf, J. (2007). Particle-size distribution as indicator for fecal bacteria contamination of drinking water from karst springs. *Environmental Science and Technology*, 41(24), 8400–8405. <https://doi.org/10.1021/es071976f>
- Raëisi, E., Groves, C., & Meiman, J. (2006). Effects of partial and full pipe flow on hydrochemographs of Logsdon river, Mammoth Cave Kentucky USA. *Journal of Hydrology*, 337(1–2), 1–10. <https://doi.org/10.1016/j.jhydrol.2006.11.015>
- Redlands, C. E. S. R. I. (2011). ArcGIS Desktop: Release (Vol. 10).
- Reimann, T., Geyer, T., Shoemaker, W. B., Liedl, R., & Sauter, M. (2011). Effects of dynamically variable saturation and matrix-conduit coupling of flow in karst aquifers. *Water Resources Research*, 47(11), W11503. <https://doi.org/10.1029/2011WR010446>
- Sánchez, D., Barberá, J. A., Mudarra, M., & Andreo, B. (2015). Hydrogeochemical tools applied to the study of carbonate aquifers: Examples from some karst systems of southern Spain. *Environmental Earth Sciences*, 74(1), 199–215. <https://doi.org/10.1007/s12665-015-4307-9>
- Shuster, E. T., & White, W. B. (1971). Seasonal fluctuations in the chemistry of limestone springs: A possible means for characterizing carbonate aquifers. *Journal of Hydrology*, 14(2), 93–128. [https://doi.org/10.1016/0022-1694\(71\)90001-1](https://doi.org/10.1016/0022-1694(71)90001-1)
- Singh, K., Malik, A., Mohan, D., & Sinha, S. (2004). Multivariate statistical techniques of the evaluation of spatial and temporal variations in water quality of Gomti river (India)—A case study. *Water Research*, 38(18), 3980–3992. <https://doi.org/10.1016/j.watres.2004.06.011>
- Stroj, A., Briški, M., & Ostrič, M. (2020). Study of groundwater flow properties in a Karst system by coupled analysis of diverse environmental tracers and discharge dynamics. *Water*, 12(9), 2442. <https://doi.org/10.3390/w12092442>
- Toran, L., & Reisch, C. E. (2013). Using stormwater hysteresis to characterize karst spring discharge. *Ground Water*, 51, 575–587.
- Vaute, L., Drogue, C., Garrelly, L., & Ghelfenstein, M. (1997). Relations between the structure of storage and the transport of chemical compounds in karstic aquifers. *Journal of Hydrology*, 199(3–4), 221–238. [https://doi.org/10.1016/S0022-1694\(96\)03245-3](https://doi.org/10.1016/S0022-1694(96)03245-3)
- Vesper, D. J., & White, W. B. (2004). Storm pulse chemographs of saturation Index and carbon dioxide pressure: Implications for Shifting recharge sources during storm events in the Karst aquifer at Fort Campbell, Kentucky/Tennessee, USA. *Hydrogeology Journal*, 12(2), 135–143. <https://doi.org/10.1007/s10040-003-0299-8>
- Vucinic, L., O'Connell, D., Teixeira, R., Coxon, C., & Gill, L. (2022). Flow cytometry and fecal indicator bacteria analyses for fingerprinting microbial pollution in karst aquifer systems. *Water Resources Research*, 58(5), e2021WR029840. <https://doi.org/10.17632/bgn5mcdj69.1>

- Vuilleumier, C., Jeannin, P. Y., Hessenauer, M., & Perrochet, P. (2021). Hydraulics and turbidity generation in the Milandre Cave (Switzerland). *Water Resources Research*, 57(8), e2020WR029550. <https://doi.org/10.1029/2020WR029550>
- Williams, P. W. (2008). The role of the epikarst in karst and cave hydrogeology: A review. *International Journal of Speleology*, 37, 1–10. <https://doi.org/10.5038/1827-806X.37.1.1>
- Winston, W. E., & Criss, R. E. (2004). Dynamic hydrologic and geochemical response in a perennial karst spring. *Water Resources Research*, 40(5). <https://doi.org/10.1029/2004WR003054>
- Worthington, S. R., & Ford, D. C. (2009). Self-organized permeability in carbonate aquifers. *Ground Water*, 47(3), 326–336. <https://doi.org/10.1111/j.1745-6584.2009.00551.x>
- Wu, Y., & Hunkeler, D. (2017). Sedimentary roles on hyporheic exchange in karst conduits at low Reynolds numbers by laboratory experiments. *Hydrogeology Journal*, 25(3), 787–798. <https://doi.org/10.1007/s10040-016-1531-7>
- Zhao, L. J., Yang, Y., Cao, J. W., Wang, Z., Luan, S., & Xia, R. Y. (2022). Applying a modified conduit flow process to understand conduit-matrix exchange of a karst aquifer. *China Geology*, 5(3), 26–33. <https://doi.org/10.31035/cg2021046>
- Zupan Hajna, N. (1992). Mineralna sestava mehanskih sedimentov in nekateri delov slovenskega kraska. *Acta Carsologica*, 21, 115–130.